Unravelling overlaps and torsion-facilitated coupling using two-dimensional laser-induced fluorescence

David J. Kemp, Adrian M. Gardner, William D. Tuttle, and Timothy G. Wright*

School of Chemistry, University of Nottingham, University Park, Nottingham NG7 2RD, UK

* Tim.Wright@nottingham.ac.uk

Abstract

Two-dimensional laser-induced fluorescence (2D-LIF) spectroscopy is employed to identify contributions to fluorescence excitation spectra that arise from both overlapping bands and coupling between zero-order states (ZOSs). Evidence is found for the role of torsional motion in facilitating the coupling between vibrations that particularly involves the lowest-wavenumber out-of-plane vibrational modes. The experiments are carried out on jet-cooled *p*-fluorotoluene, where the molecules are initially in the lowest two torsional levels. Here we concentrate on the 390–420 cm^{-1} features in the $S_1 \leftarrow S_0$ excitation spectrum, assigning the features seen in the 2D-LIF spectrum, aided by separate dispersed fluorescence spectra. The 2D-LIF spectra allow the overlapping contributions to be cleanly separated, including some that arise from vibrational-torsional coupling. Various coupling routes open up because of the different symmetries of the lowest two torsional modes; these combine with the vibrational symmetry to provide new symmetry-allowed vibration-torsion ('vibtor') interactions, and the role of the excited $m = 1$ torsional level is found to be significant.

I. Introduction

Recently, there has been a concentrated effort at understanding the interactions between vibrations and torsions in substituted benzenes, which form vibration-torsional ('vibtor') levels. Work has focused on the monomethyl molecules, toluene and *p*-fluorotoluene (*p*FT), and the dimethyl molecule, *p*-xylene (*p*Xyl). Toluene has been studied using both photoelectron spectroscopy (PES) and time-resolved PES (tr-PES), [1,2,3,4,5,6,7] zero-electron-kinetic-energy (ZEKE) spectroscopy,[6,7,8] and two-dimensional laser-induced fluorescence (2D-LIF).[9,10,11,12,13] Work has been extended to the *p*FT molecule where many of the interactions in the low-wavenumber region (< 430 cm^{-1}) of the S_1 state have been assigned employing both ZEKE[14,15] and 2D-LIF spectroscopy.[16] Earlier work includes: absorption studies by Cvitaš and Hollas[17] and Seliskar et al.;[18] LIF and dispersed fluorescence (DF) spectroscopy by Okuyama et al.,[19] Ha et al.[20] and Parmenter, Zhao et al.; [21,22,23,24] and resonance-enhanced multiphoton ionisation (REMPI) spectroscopy by Georgiev et al.[25] and Hu et al.[26], in both cases as part of a study of the *p*FT-Ar complex. Further work on higher-lying S_1 levels has been undertaken using tr-PES,[27] ZEKE[28,29] and 2D-LIF spectroscopy.[29] (A reassignment of the levels discussed in Ref. 27 has been presented in Ref. 29, and a reassignment of some of the levels discussed in Refs. 14 and 19 is presented in Refs. 15, 16 and 30.) The work of Gascooke, Lawrance and coworkers (GL) on toluene and *p*FT has provided the most-detailed description of the vibtor interactions occurring in both the S_0 and S_1 states and discussed the necessity of including such interactions in any detailed understanding of the spectroscopy of these molecules. We tackled the *p*-xylene (*p*Xyl) molecule recently[31,32] and showed that the vibtor interactions, although now involving a two-rotor system, were very similar to those of toluene and *p*FT. Overall, these vibtor interactions provide increased pathways for energy dissipation between the molecular motions and so can lead to the possibility of rapid intramolecular vibrational redistribution (IVR) at even quite low wavenumbers, and this has been compared and contrasted in recent papers focused on toluene, *p*-difluorobenzene (*p*DFB) and *p*FT,[6] as well as *p*DFB, *p*-chlorofluorobenzene (*p*ClFB), *p*FT and *p*Xyl.[33]

Recently,[29] we showed that the vibtor levels at ~845 cm^{-1} associated with the methyl torsion and the first overtone of an out-of-plane vibration in *p*FT were opening up new routes to interactions involving vibrations of different symmetry. This involved interactions between an excited torsional level of an overtone with vibtor levels formed by combinations with a set of levels at ~ 400 cm^{-1}. In the present work, we revisit those levels close to ~400 cm^{-1} in the S_1 state of *p*FT and examine the interactions using 2D-LIF spectroscopy. The present work is an extension to recently-reported work by GL,[16] which

focused on a detailed understanding of the S_1 region < 400 cm^{-1}, highlighting interactions occurring for vibtor levels involving the three lowest-wavenumber vibrations.

2. Experimental

The 2D-LIF apparatus has been described recently.[29] The vapour above room temperature *para*-fluorotoluene (99% purity, Alfa Aesar) was seeded in ~5 bar of Ar and the gaseous mixture passed through a General Valve pulsed nozzle (750 μm, 10 Hz, opening time of 180–210 μs) to create a free jet expansion. This was intersected at *X*/*D* ~20 by the frequency-doubled output of a single dye laser, operating with C540A. The fluorescence was collected, collimated and focused onto the entrance slits of a 1.5 m Czerny Turner spectrometer (Sciencetech 9150) operating in single-pass mode, dispersed by a 3600 groove/mm grating, and then ~300 cm^{-1} windows of the dispersed fluorescence were collected by a CCD camera (Andor iStar DH334T). At a fixed grating angle of the spectrometer, the wavenumber of the excitation laser was scanned, and at each excitation wavenumber the image was accumulated for 2000 laser shots. This produced a 3D surface of fluorescence intensity versus the excitation laser wavenumber and the wavenumber of the emitted and dispersed fluorescence, termed a 2D-LIF spectrum.[13]

We have also recorded separate DF spectra with higher averaging to get better signal to noise than simply taking a vertical slice through the 2D-LIF image. These DF spectra were recorded with the same spectrometer as for the 2D-LIF spectra, and were recorded three times accumulating over 5000 shots each time, and an average taken.

3. Results and discussion

3.1. Nomenclature and labelling

3.1.1. Vibrational labelling

In previous work, authors have used a combination of Wilson[34]/Varsányi[35] and Mulliken[36]/Herzberg[37] notation. As we have previously noted, Wilson notation is inappropriate because of the large change in the forms of the vibrations, from benzene to *p*FT;[38] also, the Varsányi notation is inconsistent in its treatment of different molecules (and rather confusingly also uses Wilson-type labels). We have also

pointed out[8,15] that previous usage of Mulliken labels is inconsistent as the list includes the CH_3-localised vibrations, yet the C_{2v} point group is used for the numbering. We shall comment on previous assignments alongside ours in terms of the D_i labels from Ref. 38, which are also the labels used by ourselves and GL in published work on toluene and *p*FT. (The various labels used in previous work have been included in Table 1 to aid the reader in referring between the different studies.)

Some assignments will involve vibtor levels and for these, the G_{12} molecular symmetry group (MSG) is appropriate, and so we shall use this throughout the present work. In addition, torsional levels will be labelled via their *m* quantum number, noting that the *m* number is signed, but usually only the positive value is employed. The reader may find it useful to refer to previous work[10,11,12,15,31] if they are not familiar with these labels. The correspondence between the C_{2v} point group labels and the G_{12} MSG ones are given in Table 2. To calculate the overall symmetry of a vibtor level, it is necessary to use the corresponding G_{12} label for the vibration (Table 2), and then find the direct product with the symmetry of the torsion, noting that a D_{3h} point group direct product table can be used, since the G_{12} MSG and the D_{3h} point group are isomorphic. The symmetries of the *m* levels are also given in Table 2.

Under the free-jet expansion conditions employed here, the molecules are all expected to be cooled to their zero-point vibrational level; note, however, that owing to nuclear-spin and rotational symmetry, the molecules can be in one of the $m = 0$ or $m = 1$ torsional levels.[31, 39]

3.1.2. Vibrational coupling

Each molecule has a set of vibrational normal modes that, within the harmonic approximation, constitute the various allowed coherent motions of the atoms that keep the centre of mass stationary with respect to a system of axes that rotates and translates with the molecule. In principle, the vibrations are non-interacting no matter how close the vibrations are in wavenumber, as long as we remain within the harmonic model. When comparing between similar molecules, then these normal modes might be expected to look very similar; however, it is found that the effect of changing the mass of one of the substituents can have quite a dramatic effect on the form and wavenumber of some of the vibrations. As a consequence, even within the harmonic model, the normal modes of one molecule may be quite different from those of a related one, such as between benzene and fluorobenzene,[40,41] and between benzene and *p*DFB.[38] There will then be various combination and overtone levels associated with these.

If we now include anharmonicity then, if all of the vibrational levels of a particular molecule are far enough apart in wavenumber, the interactions between them will be minimal. In this case, the eigenstates will correspond to these vibrations, each of which will be an anharmonic vibration corresponding to a particular normal mode. The difference between the well-separated anharmonic normal modes and the harmonic normal modes can be termed 'diagonal anharmonicity'. If, however, an anharmonic fundamental is close in wavenumber to one or more levels that has the same overall symmetry, then 'off-diagonal' anharmonic interactions can occur. The non-interacting levels are termed zero-order states (ZOSs), and coupling between these leads to the formation of eigenstates that are linear combinations of these, and will be at different wavenumbers to the original ZOSs.[37] This is most likely to occur when the ZOSs are energetically close together. For two interacting states, this is termed a Fermi resonance,[42] while for more than two levels we term this a complex Fermi resonance. For molecules that contain a hindered internal rotor, the ZOSs can also be torsional or vibtor levels and these can become involved in the eigenstates, thus involving further degrees of freedom. In general, these interactions lead to eigenstates that involve more widespread atomic motions and so the ZOS mixing promotes dispersal of energy through the molecule.

In electronic spectroscopy, if we assume a non-coupled picture initially, then a vibrational or vibtor ZOS can be bright (i.e. it has a significant transition intensity) or dark (i.e. it has no, or a very small transition intensity); these are often termed zero-order bright (ZOB) states and zero-order dark (ZOD) states, respectively. Following interaction, a particular eigenstate may be composed of a mixture of ZOB and ZOD state character. In the simplest case of one ZOB state interacting with one ZOD state, then two eigenstates will be formed (corresponding to a sum and difference of the ZOB and ZOD states – the classic Fermi resonance[35,42]), both of which will appear in the electronic spectrum, by virtue of the ZOB state character. Hence, as well as shifts in the observed positions of spectral lines from those expected, the interaction can give rise to the appearance of 'extra' spectral lines. In the experiments performed here, nanosecond lasers are employed, and individual eigenstates (ignoring rotational energy levels) can usually be picked out in the spectrum. By observing projections of these eigenstates onto those in another state either by DF, or by photoionisation and recording photoelectron spectra, insight into the ZOS make-up of the excited state eigenfunctions can be determined.

Such couplings are only expected to be significant for small changes, $\Delta v \leq 3$, of the vibrational quantum number, and also for changes, Δm, of 0, ±3 or ±6 in the torsional quantum number in descending order of likely strength.[11,15,31,43,44]

3.1.3. Transitions

When designating excitations, we shall generally omit the lower level, since it will be obvious from the jet-cooled conditions; similarly, for emissions, we shall omit the upper level, as that will be obvious from the excitation and context. In the usual way, vibrational transitions will be indicated by the ordinal number, *i*, of the D_i vibration, followed by the number of quanta; torsional transitions will be indicated by *m* followed by its value. Finally, vibtor transitions will be indicated by a combination of the vibrational and torsional transition labels. If no *m* values are specified, then transitions involving both *m* = 0 and *m* = 1 levels occur, whose transition wavenumbers are expected to be coincident at the present resolution. The wavenumbers of the levels will be given with respect to the relevant zero-point level in each state, but noting that some excitations will originate from the *m* = 1 level in S_0 and those transition energies are given with respect to that level, as usual. As has become common usage, we will generally refer to a level using the notation of a transition, with the level indicated by the specified quantum numbers. Also, since in the present work all of the interactions between ZOSs appear to be weak, the eigenstates are usually referred to as the overwhelmingly dominant contribution from one of the ZOSs, with the context implying if a small admixture of other ZOSs is present.

We give two examples: (i) (14^2m^0, $14_119_1m_{3(+)}$) represents an excitation from the S_0 zero-point *m* = 0 level to the *m* = 0 $2D_{14}$level in the S_1 state, followed by emission from this S_1 level to the *m* = 3(+) level of the D_{14}+D_{19} combination level in S_0; and (ii) (14^2, 9_1) represents a dual excitation from the *m* = 0 and *m*= 1 levels of the S_0 zero-point level, followed by dual emission to the corresponding *m* levels of the D_9 level in the S_0 state – note that these would be coincident with our resolution.

3.2. Overall comments on the $S_1 \leftarrow S_0$ spectrum

We have discussed the 0–830 cm^{-1} region of the $S_1 \leftarrow S_0$ excitation spectrum of *p*FT employing REMPI and ZEKE spectroscopy in our previous work.[15,28] In addition we have discussed a feature at ~845 cm^{-1} using REMPI, ZEKE and 2D-LIF spectroscopy.[29] In Figures 1(a) and 1(b) we show expanded views of the region of the 390–415 cm^{-1} region $S_1 \leftarrow S_0$ spectrum, which is the centre of attention here, recorded using both REMPI and 2D-LIF spectroscopy (integrated in the latter case – see below); it can be seen that they are very similar.

3.3. Activity expected in the 2D-LIF and DF spectra

For eigenstates that are dominated by a single ZOS, we expect to see a dominant $\Delta(v, m) = 0$ band as the strongest contributor to the fluorescence from such a level. Associated with this will be other Franck-Condon (FC)-active vibrational transitions or symmetry-allowed vibtor contributions arising from changes in geometry and/or vibrational frequencies and/or torsional potentials – for convenience, we refer to both of these as 'FC transitions' or 'FC activity' in the below. Occasionally, if there are large changes between the potentials, then it is possible that the $\Delta(v, m) = 0$ band will not be the most intense. It is possible to see weaker transitions associated with $\Delta m = \pm 3$ and, even weaker, transitions associated with $\Delta m = \pm 6$.

If an eigenstate is made up of more than one ZOS, then we expect contributions from each ZOS to appear in the spectrum. However, this assumes that there is a significant difference between the ZOS make-up of the eigenstates in both electronic states. Indeed, if the eigenstate make-up were identical in these two states, than we would just see a spectrum dominated by the $\Delta(v, m) = 0$ band corresponding to transitions between the particular eigenstate in both electronic states. Usually, however, there is a significant difference in the make-up and then for a simple Fermi resonance we would expect to see both $\Delta(v, m) = 0$ bands, with that of one ZOS dominating from one FR component, and the reverse for the second component.

In the 2D-LIF spectrum recorded across the 390–415 cm^{-1} range of excitation wavenumber (see Figure 2), we can see that there are two vertical strips of activity localised across different ranges of the excitation wavenumber. Previous ZEKE work[14] has shown that the higher-wavenumber excitation feature at 408 cm^{-1} in the REMPI/LIF spectrum in Figure 1 is largely associated with exciting 11^1, while the lower-wavenumber feature corresponds to an overlapped $14^2/29^1$ pair of transitions, with the 14^2 transition to slightly lower wavenumber. Closer inspection of the 2D-LIF spectrum in Figure 2 (and see later) indicates that indeed the lower-wavenumber vertical strip of activity is largely split into two subsets, separated in excitation wavenumber. Those slightly higher in wavenumber are consistent with being associated mainly with 29^1 and those slightly lower with 14^2. This activity will be discussed as part of the assignments below. It will also be noticed that the various bands have different profiles made up from the underlying rotational structure. Bands that are associated with a_1'' levels (such as the $m = 0$ levels of the D_{29} vibration) are of *a*-type, while those of a_1' levels (such as the $m = 0$ levels of the D_{11} vibration) are of *b*-type. [13,16] The band type may not always be obvious in cases of overlapping bands, or when rotationally-dependent interactions occur.

To identify the position of bands in the 2D-LIF spectrum in Figure 2, we refer to the pair of respective excitation and emission relative wavenumbers, with an assignment being given in terms of the pairs of respective transitions, as has been used by GL.[13,16] From these considerations, it is straightforward to identify the most intense bands in the spectrum, and these are in agreement with previous assignments.[14,15,16] The band at (399, 424) cm^{-1} is predominantly from the (29^1, 29_1) $\Delta v = 0$ transition; the band at (409, 453) cm^{-1} is associated predominantly with (11^1, 11_1); and the band at (397, 824) cm^{-1} predominantly with (14^2, 14_2). Each of these bands contains separate transitions between the respective $m = 0$ level and the $m = 1$ level associated with each vibrational state; these cannot be discerned at the present resolution. In Figures 3–5 we present DF spectra at positions that correspond to excitation of 0^0 and those corresponding to the eigenstates dominated by 14^2, 29^1 and 11^1 – noting that the 14^2 and 29^1 transitions have overlapped rotational profiles and so their separation is not wholly complete. These DF spectra are the equivalent of taking a vertical cut-through of the 2D-LIF image; however, these traces were recorded separately by averaging over a greater number of laser shots. The assignments of most of the relatively intense bands are straightforward and these are given on the figures and will be summarised briefly below. Some other more 'interesting' assignments will be discussed separately.

3.4. Assignments

3.4.1. Initial discussion

We will now give an overview of the assignments of the main transitions initially by reference to the DF spectra in Figures 3–5, obtained by exciting at the origin, 0^0, and positions corresponding to levels expected[14,15,16] to be dominated by 14^2, 29^1 and 11^1; we show the 0–1390 cm^{-1} region of the DF spectra across these figures. Later, we shall discuss some particular features of the DF and 2D-LIF spectra further, highlighting the information that can be deduced regarding any interactions between the ZOSs.

When exciting via 0^0, in the region between 0–390 cm^{-1} (see Figure 3) there is a wealth of torsional and vibtor activity in the DF spectrum that has been discussed in depth by Gascooke et al.,[16] and the reader is referred to that work. Unfortunately, the signal-to-noise is not sufficient to see any of these levels when exciting via 14^2, 29^1 or 11^1.

In the regions of the DF spectra in Figures 4 and 5, we also see bands associated with totally-symmetric, a_1' fundamentals, whose wavenumbers largely agree with those discussed and presented in Ref. 38. (Revised values for D_{20}, D_{19} and D_{30} have been presented in the 2D-LIF study of Gascooke et al.[16] and are in better agreement with the calculated values[38] than the previous ones – see Table 1.) We also see several bands that arise from Herzberg-Teller (HT) activity, and involve in-plane vibrations of a_1'' symmetry. In the region scanned, we have assigned fundamental bands associated with 29_1, 11_1, 28_1, 10_1, 9_1, 7_1, 6_1 and 5_1. We also see a number of first overtone bands associated with out-of-plane modes: 20_2, 19_2, 18_2 and 14_2. There are also a wealth of combination bands involving pairs of out-of-plane a_2' and a_2'' vibrations (and so totally-symmetric, a_1', overall). The symmetry-allowed 28_1 emission is seen following 29^1 absorption, but a band at the same wavenumber also seen when exciting 0^0. Although this could arise from similar HT activity that leads to the observation of the 29_1 emission, another possible assignment is 18_120_1.

From the above, a large number of fundamental vibrational wavenumbers in the S_0 state can be derived, and these are included in Table 1 alongside the previous experimental and calculated values. As well as these, there are various other expected combinations: for example, with 11_1 and 9_1. Clearly, to higher wavenumber more and more possibilities exist for an assignment; however, mostly a satisfactory one can be reached from earlier activity and the previous experimental and calculated values.[38] As a general point, the assignment of most bands is confirmed by their changing intensities when exciting from the different S_1 levels, so that combinations involving 11_1 are particularly strong when emitting from 11^1, for example. We also note that totally-symmetric fundamentals are particularly prominent when exciting via 0^0.

3.4.2. Main activity the 2D-LIF spectrum

We initially comment that from the section of the DF spectrum in Figure 4. We can see that when exciting to 0^0, the 11_1 band is intense, while the 29_1 band is significantly weaker, with the 14_2 band being somewhere in between. It is clear from the significant separation of the bands, that there is unlikely to be any interaction between the 29_1, 11_1 and 14_2 levels in S_0. The spectrum from 11^1 shows a strong 11_1 band, confirming its assignment; also, there is a very weak 14_2 band and no clearly discernible 29_1 band. The separate band that appears at 438 cm^{-1} is assigned as arising from 29_1m_2, which is a symmetry-allowed emission from 11^1m^1 (see later).

From 29^1 we see a strong 29_1 band in the DF spectrum in Figure 4, and although there are apparent weak 11_1 and 14_2 bands, these appear to be arising from a simultaneous excitation of 14^2 via the overlap of the rotational envelopes of the 29^1 and 14^2 bands. Lastly, from 14^2, we see a very strong 14_2 band, and a very weak 11_1 band; the significant 29_1 band appears to arise from the $14^2/29^1$ rotational envelope overlap. It is unfortunate that the partial overlap between the 29^1 and 14^2 bands obfuscates clear conclusions regarding possible interactions between the 14^2, 29^1 and 11^1 levels – further insight arises from the 2D-LIF spectra, which are now discussed in more detail.

An overview of the main 2D-LIF activity can be seen in Figure 2, but we now concentrate on expanded views of the main $\Delta(v, m) = 0$ regions, with the first focus of attention on the region shown in Figure 6. The comments above regarding the assigned activity in the DF spectra clearly also hold, but it is also apparent that there is more information in the 2D-LIF image. As presented, activity from emission to the same S_0 level appears horizontally across the 2D-LIF images, while emission to various S_0 levels from exciting a particular S_1 level appears vertically at that excitation number.

Emission activity from 11^1 is evident on the right-hand side of Figures 2 and 6, concentrated across the excitation numbers 405–410 cm^{-1} and dominated by the (11^1, 11_1) band. On the left-hand side of Figure 2, we clearly have two main subregions of emission activity, associated with exciting the level that is predominantly 29^1 and, to slightly lower wavenumber, emission from the one that is predominantly 14^2; these subregions are each dominated by their respective $\Delta(v, m) = 0$ bands. In deducing the assignments of other bands arising from emission from these upper states, we take account of the fact that such bands are expected to have a similar width of activity as the $\Delta(v, m) = 0$ band across the region. As well as (11^1, $29_1 m_2$) activity, we also see a weak but distinct ($29^1 m^2$, $29_1 m_2$) band at (412, 438) cm^{-1} in the 2D-LIF spectrum in Figure 6 together with broad activity across this region.

Immediately apparent from Figure 6 is that although there is a strong (29^1, 29_1) band, there is no clear evidence for a (11^1, 29_1) band, suggesting no significant interaction between 29^1 and 11^1, as mentioned above when discussing the DF spectra. In Figure 7 we show traces where we have integrated vertical strips of activity across the 2D-LIF spectrum for the main bands. It can be seen that there is very weak 29_1 activity in the region of 11^1, and a correspondingly small amount of 11_1 activity when exciting via 29^1. However, examining the activity at various emission wavenumbers shows that these observations are artefacts of the integrations, which are picking up some of the weak, broad activity from the main $\Delta(v, m) = 0$ bands. As a consequence, we conclude that there is no evidence for interaction between

29^1 and 11^1. Also apparent in the 2D-LIF spectrum in Figure 6 is a weak band at (399, 457) cm^{-1}; since this seems to be associated with 29^1, we assign this to the symmetry-allowed (29^1m^0, $14_1m_{3(-)}$) transition.

In Figure 8(a), we see the strong (14^2, 14_2) band, which is clearly displaced from that of the (29^1, 29_1) band, and a weak (14^2, 11_1) band. The latter is consistent with the (11^1, 14_2) band seen in this figure. These could arise from FC activity, or be evidence that the 11^1 and 14^2 levels are weakly coupled in the S_1 state; the integrated traces in Figure 7 are also consistent with these. Although the shoulder on the 29_1 trace is consistent with suggesting some 29_1 emission from 14^2, this is thought to arise from underlying rotational structure, since there is no corresponding shoulder on the low-wavenumber side of the 14_2 band, suggesting no 29_1 emission from 14^2. This is also evident in the 2D-LIF image in Figure 6, where the (29^1, 29_1) band is seen to be localised, and there is no extension of this band to lower wavenumber, as would be expected if there were a (14^2, 29_1) contribution. Overall, we conclude that there is no significant interaction between the 14^2 and 29^1 levels.

We will discuss the 489 cm^{-1} band – see Figure 6 – in Section 3.4.3.2.

As well as the three aforementioned ZOSs, in our ZEKE study[15] we deduced the involvement of another: $14^1m^{6(-)}$ and this was confirmed by Gascooke et al.[16] in their recent 2D-LIF study. In those studies, it was inferred that the 14^2m^0 and $14^1m^{6(-)}$ states were coupled. In our ZEKE study,[15] we concluded that we saw the second component of the interaction in the S_1 state at 364 cm^{-1}, but we subsequently noted[29] that unpublished 2D-LIF spectra, now reported herein, did not support this, and this is in agreement with the deductions of Gascooke et al.[16] that the interaction is very localised. We show an expanded view of this region of the 2D-LIF spectrum in Figure 9, where the ($14^1m^{6(-)}$, $14_1m_{6(-)}$) band may be clearly seen to have a rather unusual band profile, in agreement with that presented in Ref. 16, which is better resolved therein.

In Figure 10, we show an expanded view of the 2D-LIF spectrum in a region to lower wavenumber than that of Figure 2, but covering an excitation wavenumber of 0^0+364 cm^{-1}. It can be seen that there is no evidence of emission to the 618 cm^{-1} level in this region. The deduction from the ZEKE spectrum[15] arose from a ZEKE band at 538 cm^{-1} seen when exciting at 364 cm^{-1}. From Figure 10, we see that there is a 2D-LIF band at (365, 635) cm^{-1}, which can be assigned to ($14^120^1m^4$, $14_120_1m_4$), with the wavenumber of the upper state being consistent with the energy-level diagram presented in Ref. 16, and the lower level also in a reasonable position. In the cation, this level would be expected at ~ 540

cm^{-1} and so is consistent with the observed ZEKE band. Two other ZEKE bands were seen when exciting at this wavenumber. One was assigned to $30^1m^{3(+)}$, consistent with the observed 2D-LIF band seen in Ref. 16, and a second was assigned to $19^120^1m^2$. In the 2D-LIF spectrum the band at ~ (366, 501) cm^{-1} pleasingly fits the assignment as the $\Delta(v, m) = 0$ band ($19^120^1m^2$, $19_120_1m_2$).

The $14^1m^{6(-)}$ band would not be expected to be very bright exciting from a $m = 0$ 'pure' vibrational level, since $\Delta m = 6$; and indeed this band is extremely weak in the DF spectra from 0^0 (Figure 4), and not seen via 11^1. (Although it appears that there is activity to this level from 29^1, this arises from the overlapping rotational profile with 14^2.) The $14^1m^{6(-)}$ band is seen strongly from 14^2 and its intensity profile across the spectrum is very similar to that of the 14^2 band – see Figure 7, supporting the suggestion that these are intricately coupled. The overall coupling seems to be weak, however, as the two FR components are overlapped and so have not moved apart in energy; GL[16,45] have concluded that the coupling between these levels depends on the rotational levels of the two ZOSs moving in and out of resonance.

It is interesting to observe that in the S_1 state[16] the $m^{6(-)}$ and 14^1m^1 levels are close together, at 197.8 cm^{-1} and 201.4 cm^{-1}. Of course, $m^{6(-)}$ can only interact with 14^1m^0 but the corresponding band was noted as being too weak to see;[16] however, the difference in transition wavenumber is expected to be similar at ~3.6 cm^{-1}. The fact that the 14^2 and $14^1m^{6(-)}$ states are close to coincident in S_1 suggests that the interactions between ZOSs in the two different wavenumber regions are different.

3.4.3. Specific features

3.4.3.1 Additional features around the (14^2, 14_2) band. When we look at the (14^2, 14_2) $\Delta(v, m) = 0$ band in more detail – see Figure 8(b) – we can see indications of two other contributions that are located close to the 29^1 excitation energy: (399, 818) cm^{-1} (labelled A) and (399, 829) cm^{-1} (labelled B). The 14_2m_0 and 14_2m_1 origins are located at 822.8 cm^{-1} and 823.5 cm^{-1} according to GL,[16] but the two bands are not separable with our resolution. Assuming that the two extra bands indeed arise from exciting 29^1, suggested assignments are (29^1m^1, $29_130_1m_4$) and (29^1m^1, $14_129_1m_1$). These extra features are evident in Figure S4 of Ref. 16 , but the higher wavenumber emission band (A) was associated with *o*- and *m*- isomers of the ^{13}C *p*FT isotopologue, with the lower one (B) not being assigned, the profile of band A suggests the isotopomer assignment is the more reliable.[45]

Another possible source for the emission at 829 cm^{-1} (band B) would be from the $14_2m_1\ldots14_119_1m_4$ interaction in the S_0 state, analogous to the $14_1m_1\ldots19_1m_4$ interaction discussed by GL.[16]

3.4.3.2 489 cm^{-1} emission. We now consider the band at an emission wavenumber of 489 cm^{-1} – see Figure 6. The profile of this band suggests that it could be made up of two contributions: the more intense seems to be located close to the excitation profile of the (29^1, 29_1) band, while the weaker part extends across the (14^2, 14_2) region; there is only the faintest trace of activity at the 11^1 excitation position. Being so low in wavenumber, there are not too many viable $\Delta(v, m) = 0$ assignments that match both the excitation and emission wavenumbers. To this end we can rule out the following possibilities on the basis of the expected position of the S_1 level, even though the corresponding S_0 level would be at about the correct wavenumber: $20^3m^{3(-)}$, 20^1m^8, and 18^1m^1. We find we have two main contenders for a $\Delta(v, m) = 0$ band: (19^1m^5, 19_1m_5) and ($20^2m^{6(+)}$, $20_2m_{6(+)}$), which we now discuss.

The 19^1m^5 level would have the same symmetry as 29^1m^1 and so would potentially be a candidate via an interaction with that level. However, it is somewhat too low in both S_1 (expected at ~383 cm^{-1}) and S_0 (expected at ~464 cm^{-1}).[16] Hence, even though it fits (expected ~403 cm^{-1}) the ZEKE band observed at 400 cm^{-1} (Ref. 15) when exciting close to 29^1, we reject this assignment as it is expected too far away from the actual absorption and emission positions.

We would expect the $20_2m_{6(+)}$ band to appear at 492 cm^{-1}, which is in very good agreement with the observed band, and although we might expect the excitation to be at 417 cm^{-1}, GL[16] suggest this should be at ~398 cm^{-1} following vibtor coupling, which would be in line with the band's position. The associated ZEKE band would be expected at ~(222+189 = 410 cm^{-1}), and indeed we suggested this as an assignment of the observed broadish band at ~400 cm^{-1} in Ref. 15, and so $20_2m_{6(+)}$ activity is a viable contributor to the 489 cm^{-1} band. The $20^2m^{6(+)}$ level has the correct symmetry to interact with the 14^2m^0 level, which would involve a $\Delta v = 4$, $\Delta m = 6$ interaction. Hence, there is a mechanism by which the $20^2m^{6(+)}$ band can gain intensity from 14^2m^0 that is consistent with the presence of the weak part of this band at the 14^2 excitation position and the ZEKE spectrum of Ref. 15. We can then assign the brighter part of the band to the $\Delta(v, m) = 0$ transition. We thus suggest an assignment of the 489 cm^{-1} emission band to $20_2m_{6(+)}$, with intensity arising from the $14^2m^0\ldots20^2m^{6(+)}$ interaction.

3.4.3.3. 500–750 cm^{-1} bands. In Figure 9, we also see weak emissions in the range 500–600 cm^{-1} when exciting across 395–405 cm^{-1}. A very weak band at (408, 502) cm^{-1} (which is not clearly discernible in the presented figures, but can be seen in expanded versions) is likely (11^1, $11_1m_{3(+)}$), while the extremely weak (unmarked) band at (399, 522) cm^{-1} is plausibly (29^1, $19_120_1m_{3(+)}$). The DF spectrum in Figure 4 provides confirmation that there are two weak bands at (398, 538) cm^{-1} and (399, 540) cm^{-1} – see Figure 9. They have possible assignments of (14^2m^1, 14_1m_5) and (29^1m^1, 11_1m_4), respectively. We also see that there is a very weak band (not shown) in the DF spectrum at 546 cm^{-1}, seen when exciting via 11^1 and 0^0, and a likely assignment of this is to $18_1m_{3(-)}$.

The band at (399,558) cm^{-1} in Figure 9 is assigned as (29^1, 14_120_1) and is consistent with the observation of the (0^0, 14_120_1) band assigned by Gascooke et al. Although the band at (398,576) cm^{-1} could be assigned as (14^2, 20_4) or (29^1m^1, $20_129_1m_1$), it seems to be located close to centre of the $14_1m_{6(-)}$ band; additionally, the DF spectrum suggests 14^1 involvement, and so an assignment to (14^2m^1, $14_120_1m_2$) fits best. The 2D-LIF band at 600 cm^{-1} can be assigned to the totally-symmetric level $14_120_1m_{3(+)}$ – this must arise from FC activity, which is consistent with its similar profile and excitation position to the 14_2 and $14_1m_{6(-)}$ bands.

There are various assignments for the emission band at 703 cm^{-1}. A number of these can be excluded on the grounds that they do not fit the position of an expected $\Delta(v, m) = 0$ band, or are not expected to have significant FC activity: 20_3m_7, $18_1m_{6(\pm)}$, 20_4m_5, 30_2m_5 and 17_1m_2. Our favoured candidates for the emission are $14_120_2m_1$ and $14_120_2m_2$. Although the former is the best fit on the grounds of expected wavenumber, we cannot exclude the latter since there is significant lowering of some of the $m = 2$ levels in the S_1 state arising from vibtor interactions.[16]

Indeed assignment of the (397, 703) cm^{-1} band to ($14^120^2m^1$, $14_120_2m_1$) would not be consistent with the energy level diagrams presented in GL,[16] which suggests the upper level is above 420 cm^{-1} and so would not be expected at this excitation position. On the other hand, an assignment to ($14^120^2m^2$, $14_120_2m_2$) would be consistent with that work, if it is assumed there were vibtor interactions in the S_0 state that pushed the $14_120_2m_2$ level down. The $14^120^2m^2$ level would have to gain intensity from interacting with 29^1m^1, which both have *e*′ symmetry. Indeed, the 2D-LIF spectrum in Figure 9 shows weak 703 cm^{-1} emission across the 29^1m^1 excitation region. We currently favour the assignment of the more intense part of the 703 cm^{-1} band to emission to $14^120^2m^2 \ldots 29^1m^1$, with the weaker part to $29^1m^1 \ldots 14^120^2m^2$.

We do, however, wish to comment that if further interactions to those considered in Ref. 16 occurred in the S_1 state, then this may cause the ($14^1 20^2 m^1$, $14_1 20_2 m_1$) to become a viable assignment on energetic grounds; however, it would still be necessary to explain how the upper state gained intensity. An interaction with $14^2 m^1$ is symmetry allowed, but the usual anharmonic and torsional coupling terms would not lead to such coupling, and so it would be necessary to invoke either an indirect coupling route (and it is unclear what this would be), Coriolis-type coupling via the involvement of rotations, or to invoke a new coupling term, possibly arising from the distortion of the torsional potential as a result of the angular variation of the interaction with the vibrational motion. Interestingly, we also see emission at ~700 cm^{-1} when exciting at 365 cm^{-1}, Figure 10, which could suggest a ($14^1 20^1 m^4$, $14_1 20_2 m_1$) symmetry-allowed assignment, or the less-likely ($14^1 20^1 m^4$, $14_1 20_2 m_2$), which would have to be vibronically induced and also involve Δm = 6. There is also weak activity at (412, 703) cm^{-1}, which could be assigned to the symmetry-allowed Δm = 3 transition ($29^1 m^2$, $14_1 20_2 m_1$). We also note that there is some evidence for activity of $14^1 20^2 m^1$ in absorption from the ZEKE spectra published in Ref. 15, where a weak band is seen at 572 cm^{-1} when exciting around the 14^2 position (in the absence of further shifts from vibtor interactions, this band would be too low in wavenumber to arise from $14^1 20^2 m^2$). Overall, however, the rationale for any such activity of the $14^1 20^2 m^1$ activity is elusive. If the corresponding m = 1 and m = 2 levels were degenerate in S_1, this might also explain the observations if there were different transition intensities for these. As such, we cannot firmly decide on the complete assignment of the 703 cm^{-1} band, but have concluded it arises from emission to $14_1 20_2 m_x$ (x = 1 and/or 2) level, with the corresponding S_1 levels interacting with either $14^2 m^1$ or $29^1 m^1$, as discussed.

Finally, the (399, 713) cm^{-1} band can be assigned to (29^1, $20_2 29_1$), and the band at (409,743) cm^{-1} is straightforwardly assigned as (11^1, $11_1 20_2$).

3.4.3.4. Comments on bands 750–920 cm^{-1}. We now return to the region of the 2D-LIF spectrum shown in Figure 8(a). The weak band at (398,766) cm^{-1} is aligned with the 14_2 band and the best assignment we have found is (14^2, $14_1 30_1 m_{3(-)}$), while the band at (399,777) cm^{-1} is located at the position of 29^1 and so is plausibly ($29^1 m^0$, $10_1 m_{3(+)}$). The 2D-LIF band at 800 cm^{-1} appears to arise from FC activity and have a similar profile and position to the 14_2 and $14_1 m_{6(-)}$ bands, a reasonable assignment involving totally-symmetric levels is ($14^2 m^0$, $14_1 19_1 m_{3(+)}$)

Both (14^2, 9_1) and (11^1, 9^1) bands, and possibly a very weak (29^1, 9_1) band, are seen in the spectrum. Interestingly, there is a clear (29^1, 29_2) band, even though it is symmetry forbidden and so suggesting

HT activity. There is also a (11^1, 29_2) band, which is very weak, even though it is symmetry allowed; there is, however, no definitive evidence of a (14^2, 29_2) band. At (399, 879) cm^{-1} is the clear (29^1, 11_129_1) band, and there also seems to be a very faint (11^1, 11_129_1) band, which is easier to discern in the DF spectrum (Figure 4); this could be indicative of very weak HT activity between 11^1 and 29^1, with the band intensity enhanced because of the excitation at the 11^1 position. There is also a significant (11^1, 11_2) band, which may have a much weaker (14^2, 11_2) FC-active counterpart, but the latter could also arise from a contribution from $20_214_1m_{6(-)}$.

3.4.3.5 Comments on bands 920–1150 cm^{-1}. In Figure 11 we show an expanded view of the 2D-LIF spectrum covering the range (390–415, 940–1150) cm^{-1}. A very weak band at (399, 943 cm^{-1}) seems likely to be associated with 11_1 and the level that gives rise to the 489 cm^{-1} band – see Section 3.4.3.2 – and hence be ($20^2m^{6(+)}$, $11_120_2m_{6(+)}$). A very weak band at (398, 990) cm^{-1} is potentially the (14^2m^1, $14_118_1m_4$) band.

The symmetry-forbidden (29^1, 28_129_1) band is present at (399, 1062) cm^{-1}, and ties in with the 29_1, 28_1 and 29_2 activity at this excitation position. The band at (398, 1071) cm^{-1} can be associated with emission to $11_114_1m_{6(-)}$ as the band profile closely matches that of the (398, 618) cm^{-1} band associated with emission to $14_1m_{6(-)}$, discussed in Section 3.4.2.

There are two bands associated with emission at 1091 cm^{-1}, appearing when exciting 29^1 and 11^1 positions. The (399, 1091) cm^{-1} band can be straightforwardly assigned as (29^1, 11_128_1), but since we do not see a significant (11^1, 28_1) band and also as the (11^1, 11_129_1) bands were weak, this suggests that the (409, 1091) cm^{-1} band is unlikely to be (11^1, 11_128_1). Our favoured assignment is to $11_118_120_1$. Particularly as the band profiles look to be different, and the centres of the bands are at slightly different emission wavenumbers. Although there is only the slightest trace of the 18_120_1 band that is expected to appear at ~(409, 640) cm^{-1}, it is likely that the (11^1, $11_118_120_1$) band is enhanced by the 11_1 character when exciting at 11^1, as seen for many bands in the DF spectra in Figures 4 and 5.

There is a very weak band at (397, 1110) cm^{-1} that is assignable to (14^2, 14_220_2); an exceptionally weak band at (409, 1119) cm^{-1} that is assignable as (11^1, 11_119_2) and a weak band at (398, 1129) cm^{-1} that is assignable as (14^2, 9_120_2).

3.4.3.6 Bands to higher wavenumber. In Figure 12 we show the region of the 2D-LIF spectrum associated with a higher excitation wavenumber. Several very weak bands appear, whose assignments

can be deduced as follows, based on the agreement of their positions with both the expected excitation and emission wavenumbers.

The band at (438, 513) cm^{-1} is assigned to (18^1m^2, 18_1m_2). There are two plausible assignments of the band at (451, 452) cm^{-1}, (30^1m^5, 30_1m_5) and ($m^{9\pm}$, $m_{9\pm}$), but a definitive assignment is not possible at this time. The band at (463, 544) cm^{-1} seems likely to be ($18^1m^{3(-)}$, $18_1m_{3(-)}$). The feature at (482, 668) cm^{-1} was assigned to (19^2, 19_2), by GL,[16] with which we concur. They saw a separation of the m = 0 and m = 1 components, which is just about discernible in expanded views of our image. Finally, the band at (494, 668) cm^{-1} is assigned to the $\Delta(v, m) = 0$ transition, ($19^120^2m^{3(-)}$, $19_120_2m_{3(-)}$).

To higher wavenumber in the DF spectra (Figures 4 and 5) we see some other features. The DF band at 1071 cm^{-1} (Figure 4) is assigned as $11_114_1m_{6(-)}$ with its band shape and location consistent with that of the 618 cm^{-1} band assigned as emission to $14_1m_{6(-)}$. In Figure 4, we see the 18_2 band at 1000 cm^{-1}, with transitions involving the D_{18} overtone being the subject of our recent paper using ZEKE and 2D-LIF spectroscopy.[29] The three intense DF bands at 1215 cm^{-1}, 1228 cm^{-1} and 1241 cm^{-1} (Figure 5) can be assigned as 6_1, 13_114_1 and 5_1, respectively, with the middle band providing a value for D_{13} in the S_0 state, which is included in Table 1. Lastly, we mention the 11_3 DF band, which appears when exciting via 11_1, concomitant with the strong enhancements of 11_1 and 11_2 via the 11^1 excitation (Figures 4 and 5). The 11^n progression seems very harmonic – consistent with at most a weak interaction of 11^1 with 14^2.

IV. Final remarks and conclusions

We have presented a wide region of the 2D-LIF spectrum, and separately-recorded associated DF spectra, across excitation wavenumbers 360–430 cm^{-1}. These have revealed a wealth of underlying structure and the activity has provided insight into the activity of different S_1 ZOSs. The results are significant since they reveal extensive vibration-torsion activity. We have seen the fundamentals 29_1, 28_1, 11_1, 10_1, 9_1, 7_1, 6_1 and 5_1 giving gas-phase values for the corresponding vibrations, and also for the S_0 D_{13} mode via the 13_114_1 combination band, and these are all included in Table 1.

Comparison of the different DF spectra in Figures 4 and 5 show that the changing relative intensities of the bands across the spectra are a powerful confirmation of many of their assignments. The DF bands from 790–890 cm^{-1} are a case in point (see Figure 4) where the changing activities are very profound: the 9_1 band dominates the spectrum via the origin, but is extremely weak via 29^1; also there appears to be little correspondence in the profiles of the 9_1 and 29_2 bands in the S_0 state. The fact that 29_2 is very weak via 14^2 suggests that the 29_2 band seen when exciting via 29^1 is likely HT activity, rather than a result of any $14^2 \ldots 29^1$ interaction or overlap in band profiles.

Indeed, we find little evidence that there is any significant interaction between the 14^2, 29^1 and 11^1 levels. The 2D-LIF and DF spectra show evidence of weak cross activity between 11^1 and 14^2, but this could simply be FC activity. We have previously concluded that these levels are close to coincident in the *p*ClFB molecule,[46] but that there was no clear evidence of interaction from the ZEKE spectra reported therein. In *p*FT, we have seen herein that there is also little evidence for any significant interaction between these two levels, which is in agreement with the results of our ZEKE study.[15] Symmetry suggests that cross activity between the 29^1 and 14^2 levels could occur as a result of HT coupling, which would be strongly dependent on the relative energies of the electronic states involved, and so vary from molecule to molecule; another possibility is rotation-induced coupling such as suggested for the $14^2m^0 \ldots 14^1m^{6(-)}$ interaction.[16,45] This would be a Coriolis-like interaction, but with its efficiency also expected to be strongly dependent on rotational levels coming in and out of resonance, and would be expected to be more prevalent at higher temperatures. Since we are working under jet-cooled conditions, the requirement for resonance would be more pronounced. However, currently there is little evidence from the spectra to infer that there is any significant cross activity between the 29^1 and 14^2 levels, which therefore excludes significant coupling of these levels. As a consequence, we conclude that each of the three states, 11^1, 29^1 and 14^2 are inherently 'bright', again in agreement with conclusions we have made in other work on *p*FT and related molecules.[8,15,33,46]

We have previously discussed in depth[29] a feature that appears at S_1+845 cm^{-1} and the interactions there were isolated to the 18^2m^1 level, which allowed couplings to vibtor combinations involving m = 2. In so-doing, the mechanism opens up couplings between vibrations of different symmetry; such is also included in the vibtor coupling of the three lowest-wavenumber vibrations included in the model of GL.[16] In our recent study of the S_1 0^0+ 845 cm^{-1} band,[29] the 18^2m^1 ZOB state was concluded as interacting with combinations formed from the 18^1m^2 vibtor level with each of the 14^2, 29^1 and 11^1 levels, which are part of the present work. Pairwise interactions with the ZOB state occurred and it was possible that weak interactions between the so-formed eigenstates was also present, although a

clear interpretation was hindered by further dissipative IVR processes. Thus, that work would be consistent with the at most weak interactions between the 14^2, 29^1 and 11^1 ZOSs concluded in the present work, taking on board that the ZOS separations and couplings will not be identical to those in the combination bands.

A significant interaction does occur between 14^2 and $14^1m^{6(-)}$, which has been suggested[16,45] as occurring via vibration-torsion-rotational coupling; additionally we have concluded that there is a possible interaction between 14^2m^0 and $20^2m^{6(+)}$. Frustratingly, the appearance of the 703 cm^{-1} emission band suggests that there may be an interaction between 14^2m^1 and $14^120^2m^1$, but the mechanism for this is unclear, but could be vibrational-rotational (Coriolis) in origin, but we currently favour the $14^120^2m^2\ldots29^1m^1$ interaction. Moreover, we particularly highlight the appearance of many vibtor bands that have activity involving 14_1 when exciting via 14^2, with a number of these also involving combinations with 20_1, such as $14_120_1m_2$ at 576 cm^{-1}, $14_120_1m_{3(+)}$ at 600 cm^{-1} $14_120_1m_4$ at 634 cm^{-1}, $14_120_2m_1$ at 703 cm^{-1}, as well as $14_119_1m_{3(+)}$ at 800 cm^{-1}. We explicitly note that the transitions involving m_1 and m_2 and m_4 must originate from 14^2m^1, while transitions involving m_0, $m_{3(+)}$ and $m_{6(\pm)}$ must originate from 14^2m^0. Further, we have seen that the 29_1m_2 level is active when exciting via 11^1 and suggests an interaction between the 29^1m^2 and 11^1m^1 levels. Overall, there is compelling evidence for the involvement of the m^1 torsional level in promoting activity through vibration-torsion coupling mechanisms. In principle, if the band centres can be precisely determined, then quantitative information on the interactions between the various levels can be extracted from the spectra, as done by GL recently,[16] although all pertinent levels would ideally be observed. It is also possible to calculate the interactions using quantum chemistry, but this would require reliable anharmonic couplings and/or van der Waals interactions to be calculated. Both of these are challenging, particularly in the S_1 state, where the out-of-plane vibrations prove to be challenging.[15,28]

That we see significant couplings at these very low wavenumbers is, of course, unusual. In Ref. 33 we have explicitly looked at the density of states, comparing *p*ClFB, *p*FT, *p*DFB and *p*Xyl. There we saw that there was a very erratic build-up in the density of states of 'pure' vibrational levels that did not differ too much for each of the molecules at < 1000 cm^{-1}; however, there was a dramatic increase in the DOS once vibtor levels were included, but the build-up is still erratic at very low wavenumbers. It is becoming indisputable that there is clear evidence for the methyl rotor having a dramatic direct impact on the make-up of the energy levels of molecules, and that this impacts on the couplings between these and so, as a consequence, on photophysical and photochemical behaviour.

Acknowledgements

We are grateful to the EPSRC for funding (grant EP/L021366/1) and to the High Performance Computer resource at the University of Nottingham. The EPSRC and the University of Nottingham are thanked for a studentship to D.J.K. We note that Lewis Warner (Royal Society of Chemistry Summer Bursary student) helped in the recording of several dispersed fluorescence spectra. We acknowledge extremely useful discussions with Warren Lawrance and Jason Gascooke (Flinders, Adelaide) and thank them for sharing unpublished data and clarifying some aspects of vibration-torsional coupling.

Conflicts of interest

There are no conflicts to declare.

Reference

[1] S. M. Bellm, P. T. Whiteside, and K. L. Reid, J. Phys. Chem. A **107**, 7373 (2003).

[2] P. T. Whiteside, A. K. King, and K. L. Reid, J. Chem. Phys. **123**, 204316 (2005).

[3] P. T. Whiteside, A. K. King, J. A. Davies, K. L. Reid, M. Towrie, and P. Matousek, J. Chem. Phys. **123**, 204317 (2005).

[4] C. J. Hammond, K. L. Reid, and K. L. Ronayne, J. Chem. Phys. **124**, 201102 (2006).

[5] J. A. Davies, A. M. Green, and K. L. Reid, Phys. Chem. Chem. Phys. **12**, 9872 (2010).

[6] J. A. Davies, A. M. Green, A. M. Gardner, C. D. Withers, T. G. Wright, and K. L. Reid, Phys. Chem. Chem. Phys. **16**, 430 (2014).

[7] A. M. Gardner, A. M. Green, V. M. Tamé-Reyes, K. L. Reid, J. A. Davies, V. H. K. Parkes, and T. G. Wright, J. Chem. Phys. **140**, 114308 (2014).

[8] A. M. Gardner, A. M. Green, V. M. Tamé-Reyes, V. H. K. Wilton, and T. G. Wright, J. Chem. Phys. **138**, 134303 (2013).

[9] E. A. Virgo, J. R. Gascooke, and W. D. Lawrance, J. Chem. Phys. **140**, 154310 (2014).

[10] J. R. Gascooke, E. A. Virgo, and W. D. Lawrance, J. Chem. Phys. **142**, 024315 (2015).

[11] J. R. Gascooke, E. A. Virgo, and W. D. Lawrance, J. Chem. Phys. **143**, 044313 (2015).

[12] J. R. Gascooke and W. D. Lawrance, J. Molec. Spec. **318**, 53 (2015).

[13] J. R. Gascooke and W. D. Lawrance, Eur. Phys. J. D **71**, 287 (2017).

[14] V. L. Ayles, C. J. Hammond, D. E. Bergeron, O. J. Richards, and T. G. Wright, J. Chem. Phys. **126**, 244304 (2007).

[15] A. M. Gardner, W. D. Tuttle, L. Whalley, A. Claydon, J. H. Carter, and T. G. Wright, J. Chem. Phys. **145**, 124307 (2016).

[16] J. R. Gascooke, L. D. Stuart, P. G. Sibley, and W. D. Lawrance, J. Chem. Phys. **149**, 074301 (2018). This work contains considerable extra information in its supplementary information. Note, however, that the excitation wavenumber axis is incorrect in Figure S9.

[17] T. Cvitaš and J. M. Hollas, Molec. Phys. **20**, 645 (1971).

[18] C. J. Seliskar, M. A. Leugers, M. Heaven, and J. L. Hardwick, J. Mol. Spect. **106**, 330 (1984).

[19] K. Okuyama, N. Mikami, and M. Ito, J. Phys. Chem. **89**, 5617 (1985).

[20] Y. M. Ha, I. S. Choi, and S. K. Lee, Bull. Kor. Chem. Soc. **19**, 202 (1998).

[21] Z.-Q. Zhao and C. S. Parmenter, *Mode Selective Chemistry* (Kluwer, 1991) Eds. J. Jortner, R. D. Levine, and B. Pullman. Jerusalem Symp. Quant. Chem. Biochem. **24**, 127 (1991).

[22] Z.-Q. Zhao, C. S. Parmenter, D. B. Moss, A. J. Bradley, A. E. W. Knight, and K. G. Owens, J. Chem. Phys. **96**, 6362 (1992).

[23] Z.-Q. Zhao, PhD Thesis, Indiana University (1992).

[24] Q. Ju, C. S. Parmenter, T. A. Stone, and Z.-Q. Zhao, Isr. J. Chem. **37**, 379 (1997).

[25] S. Georgiev, T. Chakraborty, and H. J. Neusser, J. Phys. Chem. A **108**, 3304 (2004).

[26] Y. Hu, X. Wang, and S. Yang, Chem. Phys **290**, 233 (2003).

[27] J. A. Davies and K. L. Reid, J. Chem. Phys., 2011, **135**, 124305.

[28] W. D. Tuttle, A. M. Gardner, L. E. Whalley, and T. G. Wright, J. Chem. Phys. **146**, 244310 (2017).

[29] A. M. Gardner, W. D. Tuttle, L. E. Whalley, and T. G. Wright, Chem. Sci. **9**, 2270 (2018).

[30] Z.-Q. Zhao, PhD Thesis, Indiana University (1992).

[31] A. M. Gardner, W. D. Tuttle, P. Groner, and T. G. Wright, J. Chem. Phys. **146**, 124308 (2017).

[32] W. D. Tuttle, A. M. Gardner, K. B. O'Regan, W. Malewicz, and T. G. Wright, J. Chem. Phys. **146**, 124309 (2017).

[33] W. D. Tuttle, A. M. Gardner, L. E. Whalley, D. J. Kemp, and T. G. Wright, Phys. Chem. Chem. Phys. In Press. (2019) DOI: 10.1039/c8cp02757a

[34] E. B. Wilson, Jr, Phys. Rev. 45 (1934) 706.

[35] G. Varsányi, *Assignments of the Vibrational Spectra of Seven Hundred Benzene Derivatives* (Wiley, New York, 1974).

[36] R. S. Mulliken, J. Chem. Phys. **23**, 1997 (1955).

[37] G. Herzberg, Molecular Spectra and Molecular Structure II. Infrared and Raman Spectra of Polyatomic Molecules (Krieger, Malabar, 1991).

[38] A. Andrejeva, A. M. Gardner, W. D. Tuttle, and T. G. Wright, J. Molec. Spectrosc. **321**, 28 (2016).

[39] P. J. Breen, J. A. Warren, E. R. Bernstein, and J. I. Seeman, J. Chem. Phys. **87**, 1917 (1987).

[40] I. Pugliesi, N. M. Tonge, and M. C. R. Cockett, J. Chem. Phys. **129**, 104303 (2008).

[41] A. M. Gardner and T. G. Wright, J. Chem. Phys. **135**, 114305 (2011).

[42] E. Fermi, Z. Phys. **71**, 250 (1931).

[43] J. R. Gascooke and W. D. Lawrance, *J. Chem. Phys*., 2013, **138**, 134302.

[44] N. T. Whetton and W. D. Lawrance, *J. Phys. Chem.*, 1989, **93**, 5377–5384.

[45] J. R. Gascooke and W. D. Lawrance, unpublished work.

[46] D. J. Kemp, L. E. Whalley, W. D. Tuttle, A. M. Gardner, B. T. Speake, and T. G. Wright, Phys. Chem. Chem. Phys. **20**, 12503 (2018).

Table 1: Calculated and experimental vibrational wavenumbers (cm^{-1}) for the S_0, S_1 and D_0^+ electronic states of *p*FT.[a]

		Wilson/ Varsányi		S_0		S_1		D_0^+	
D_i[b]	Mulliken[c] 'C_{2v}'	Ref. 14	Duschinsky[d]	B3LYP[e]	Expt[f]	B3LYP[g]	Expt[h]	B3LYP[i]	Expt[j]
a_1'									
D_1	1	2	**2**,7a	3103	3068	3130		3116	
D_2	2	20a	**13**,20a	3071	3068	3105		3101	
D_3	4	8a	**9a**	1598	1603	1528		1628	1631
D_4	5	19a	**18a**,(20a)	1499	1513	1432		1454	
D_5	7	7a	1,7a,(2,6a)	1209	1241[k]	1213	1230	1311	1332
D_6	8	13	12,19a,20a,(13 18a)	1192	1215[k]	1185	1194	1211	1230
D_7	9	9a	**8a**	1145	1159[k]	1120		1158	1170
D_8	10	18a	**19a**,12	1005	1001	954		969	
D_9	11	1	**1**,6a,(7a,2)	827	843[l]	805	797	811	824
D_{10}	12	12	20a,12,(19a,13)	715	730[k]	700	711	710	721
D_{11}	13			446	453[l]	410	408[l]	437	440
a_2'									
D_{12}	14	17a	**17a**	953	956	588	618	987	985
D_{13}	15	10a	**10a**	808	810	484	512	770	777
D_{14}	16	16a	**16a**	418	414[l]	172	199[l]	356	350
a_2''									
D_{15}	20	5	**5**,10b	931	929	706	678	998	1008
D_{16}	21	17b	**17b**,11,(16b)	817	819	651	607	832	842
D_{17}	22	4	**4**,(10b)	698	695	538	509	671	685
D_{18}	23	16b	**16b**,11,(17b)	500	500[k]	468	426	488	499
D_{19}	24	10b	**10b**,(4,5)	330	334[l]	243	239[l]	266	271
D_{20}	25	11	16b,17b,11	141	143[l]	110	104[l]	109	111
a_1''									
D_{21}	26	7b	**20b**	3102	3040	3126		3115	
D_{22}	27	20b	**7b**	3071	3040	3100		3101	
D_{23}	29	8b	**9b**	1586	1592	1427		1383	
D_{24}	31	19b	**18b**,(19b,14,15)	1395	1435	1315		1470	
D_{25}	32	14	**15**,(14)	1283	1300	935		1301	
D_{26}	33	3	**3**,8b	1292	1321	1255		1250	
D_{27}	34	18b	**14**,19b	1090	1099	1053		1115	
D_{28}	36	6b	**6b**,(8b)	633	640[l]	546	552	564	570
D_{29}	37	9b	8b,6b,(3)	414	424[l]	395	399[l]	412	416
D_{30}	38	15	19b,14,(18b)	298	307[l]	307	309[l]	313	320

[a] Symmetries of the vibrations are given in the G_{12} molecular symmetry group.

[b] See Ref. 38 for a discussion of these labels and to see mode diagrams.

[c] Used in Ref. 14 and related work – these are rather misleading labels, as the numbering included the vibrations of the methyl group, which cannot be described in C_{2v}.

[d] These express the S_0 modes of *p*FT in terms of those of benzene, using a generalised Duschinsky approach involving artificial isotopologues – see Ref. 38. Values outside parentheses have mixing coefficients > 0.2 and are termed major contributions, with bolded values being dominant contributions (mixing coefficients > 0.5). Those inside parentheses are minor contributions, and have values between 0.05 and 0.2. If there is more than one contribution of each type, these are given in contribution order. Vibrations with a mixing coefficient < 0.05 are ignored.

[e] B3LYP/aug-cc-pVTZ – see Ref. 38.

[f] From Ref. 38 unless otherwise noted. See that work for a discussion of the assignments and references to original papers.

[g] TD-B3LYP/aug-cc-pVTZ – see Ref. 28.

[h] From Ref. 28 unless otherwise noted.

[i] UB3LYP/aug-cc-pVTZ – see Ref. 28.

[j] From Refs. 14, 15 and 28

[k] From present work.

[l] From Ref. 16 and consistent with Ref. 28 and present work.

Table 2: Correspondence of the C_{2v} point group symmetry classes with those of the G_{12} molecular symmetry group. Also indicated are the symmetries of the different pure torsional levels.[a]

C_{2v}	G_{12}	m
a_1	a_1'	0, 6(+)
a_2	a_2'	6(-)
b_1	a_2''	3(-)
b_2	a_1''	3(+)
	e'	2,4
	e''	1,5

[a] Symmetries of vibtor levels can be obtained by combining the vibrational symmetry (in G_{12}) with those of the pure torsional level, using the direct product table of the isomorphic D_{3h} point group. Vibrational symmetries are given in Table 1.

Figure 1

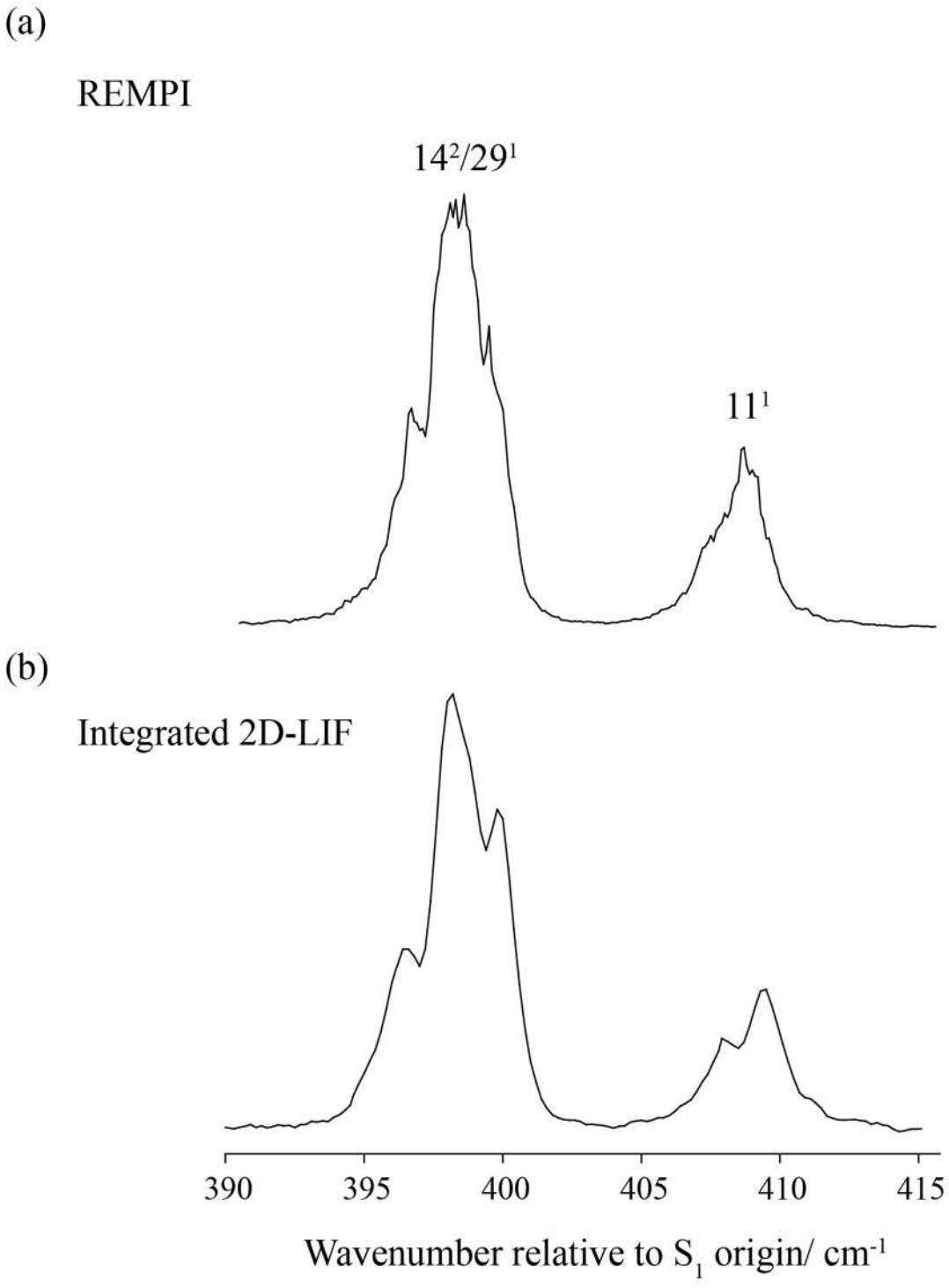
(a)
REMPI
$14^2/29^1$
11^1
(b)
Integrated 2D-LIF
390
395
400
405
410
415
Wavenumber relative to S_1 origin/ cm^{-1}

Figure 2

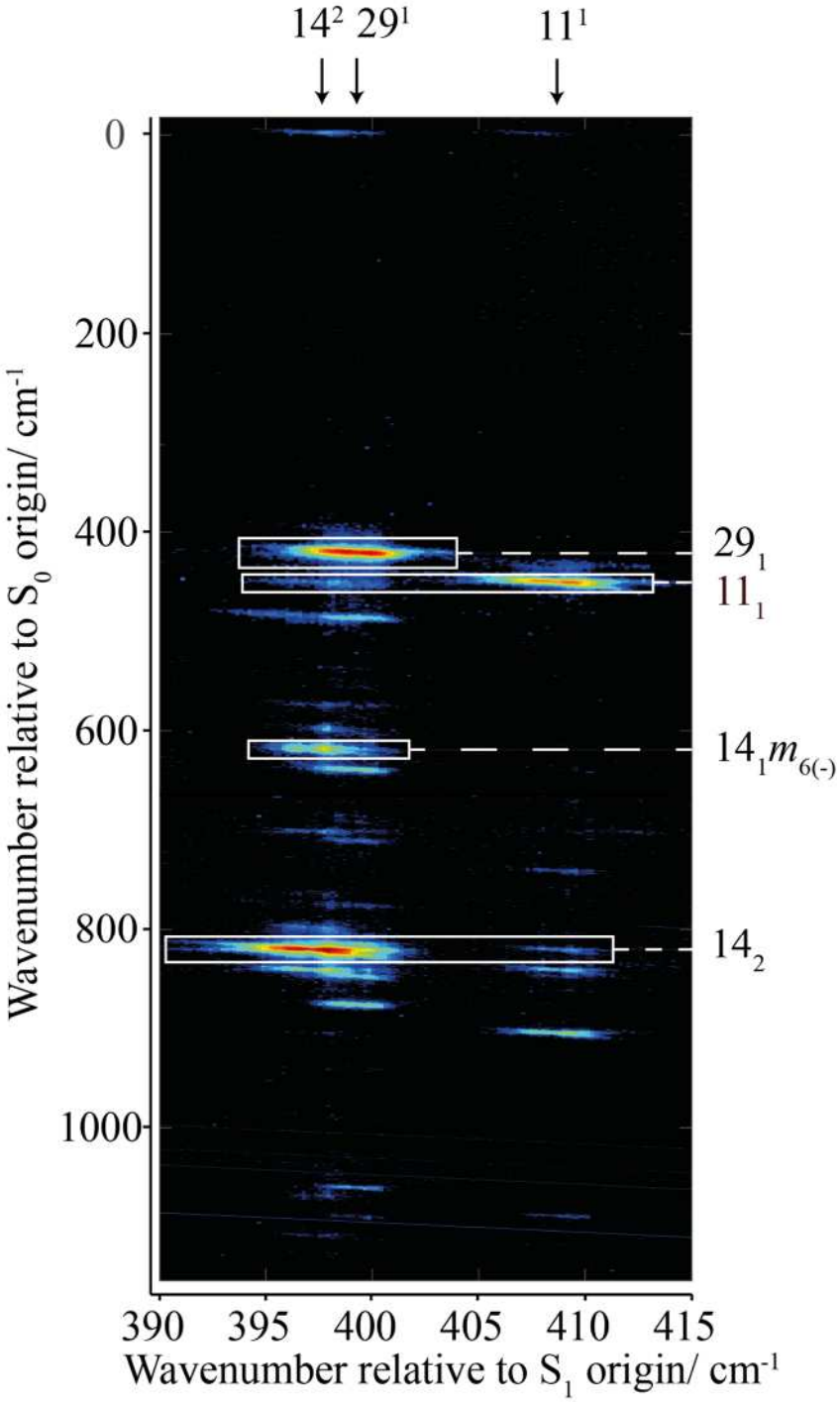
14^2 29^1
11^1
0
200
400
600
800
1000
Wavenumber relative to S_0 origin/ cm^{-1}
29_1
11_1
$14_1 m_{6(-)}$
14_2
390
395
400
405
410
415
Wavenumber relative to S_1 origin/ cm^{-1}

Figure 3

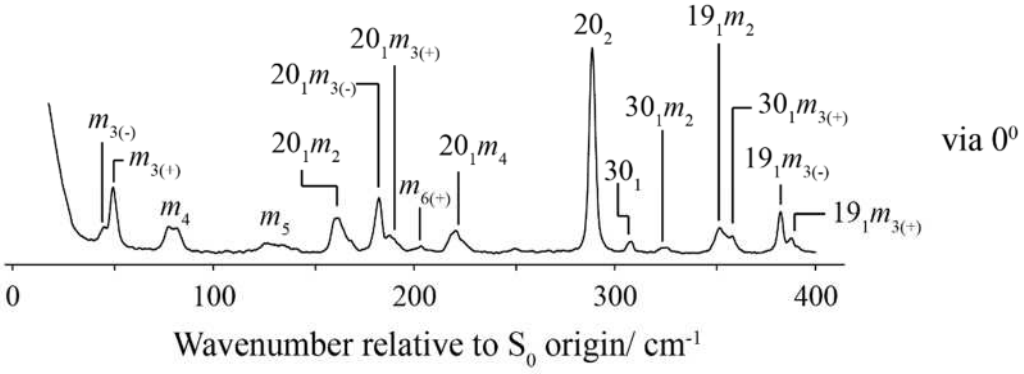
$m_{3(-)}$
$m_{3(+)}$
m_4
m_5
20_1m_2
$20_1m_{3(-)}$
$20_1m_{3(+)}$
$m_{6(+)}$
20_1m_4
20_2
30_1
30_1m_2
19_1m_2
$19_1m_{3(-)}$
$30_1m_{3(+)}$
$19_1m_{3(+)}$
via 0^0
0
100
200
300
400
Wavenumber relative to S_0 origin/ cm^{-1}

Figure 4

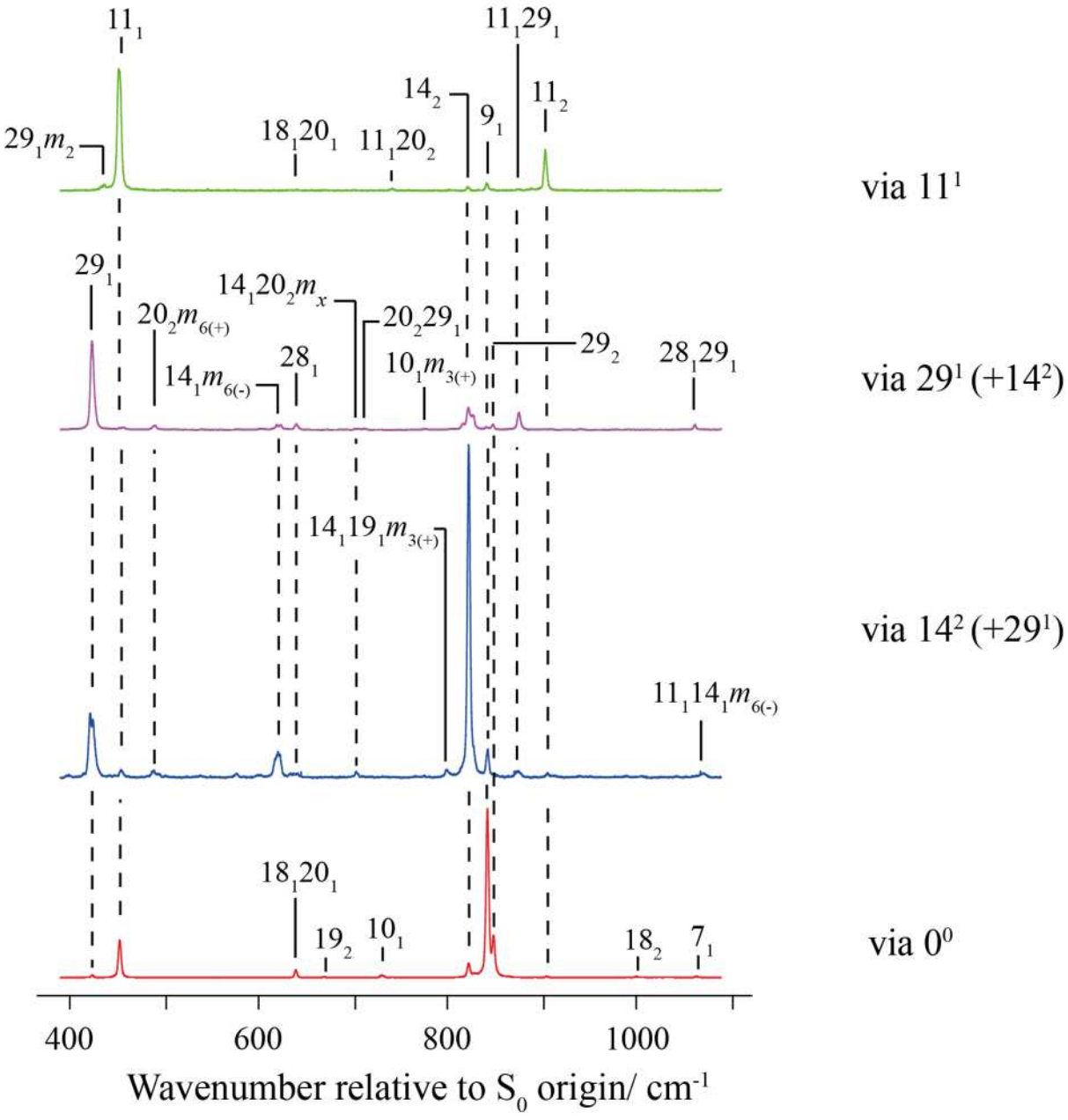
11_1
$11_1 29_1$
14_2
11_2
$29_1 m_2$
$18_1 20_1$
$11_1 20_2$
9_1
via 11^1
29_1
$14_1 20_2 m_x$
$20_2 m_{6(+)}$
$20_2 29_1$
29_2
$28_1 29_1$
$14_1 m_{6(-)}$
28_1
$10_1 m_{3(+)}$
via 29^1 (+14^2)
$14_1 19_1 m_{3(+)}$
$11_1 14_1 m_{6(-)}$
via 14^2 (+29^1)
$18_1 20_1$
19_2
10_1
18_2
7_1
via 0^0
400
600
800
1000
Wavenumber relative to S_0 origin/ cm^{-1}

Figure 5

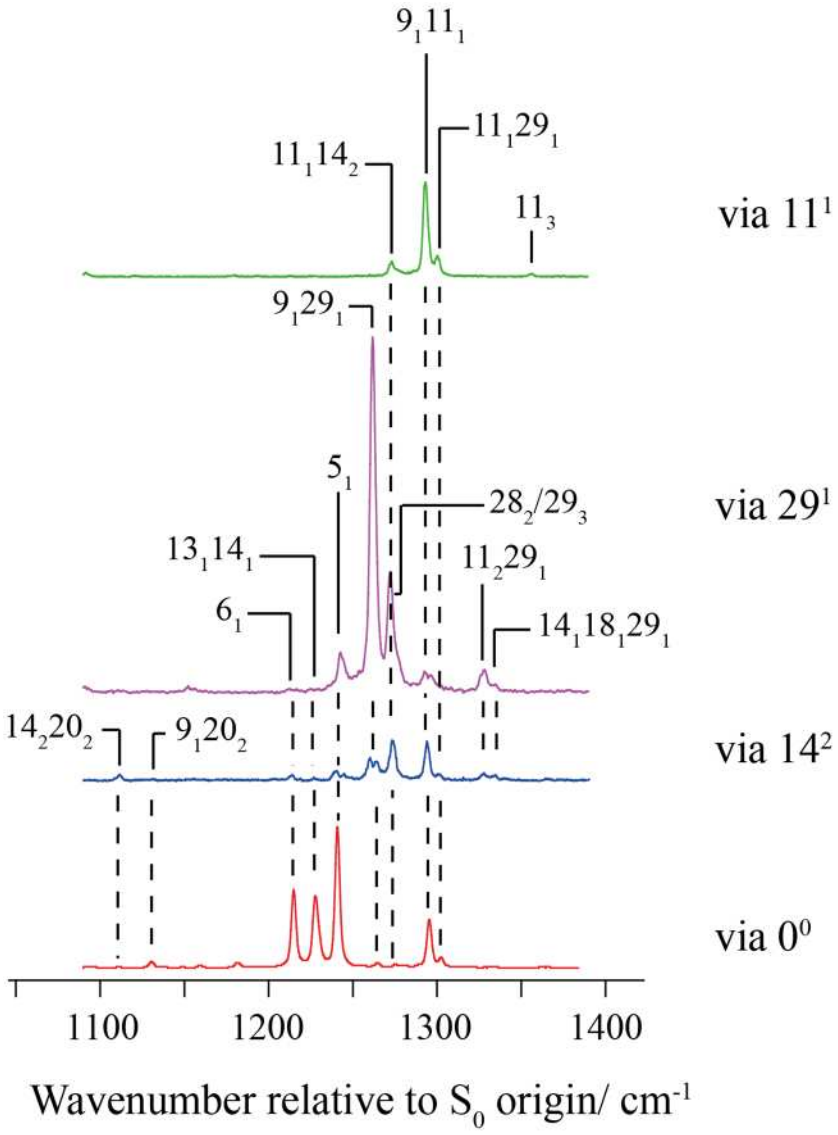
9₁11₁
11₁29₁
11₁14₂
11₃
via 11¹
9₁29₁
5₁
28₂/29₃
via 29¹
13₁14₁
11₂29₁
6₁
14₁18₁29₁
14₂20₂
9₁20₂
via 14²
via 0⁰
1100
1200
1300
1400
Wavenumber relative to S₀ origin/ cm⁻¹

Figure 6

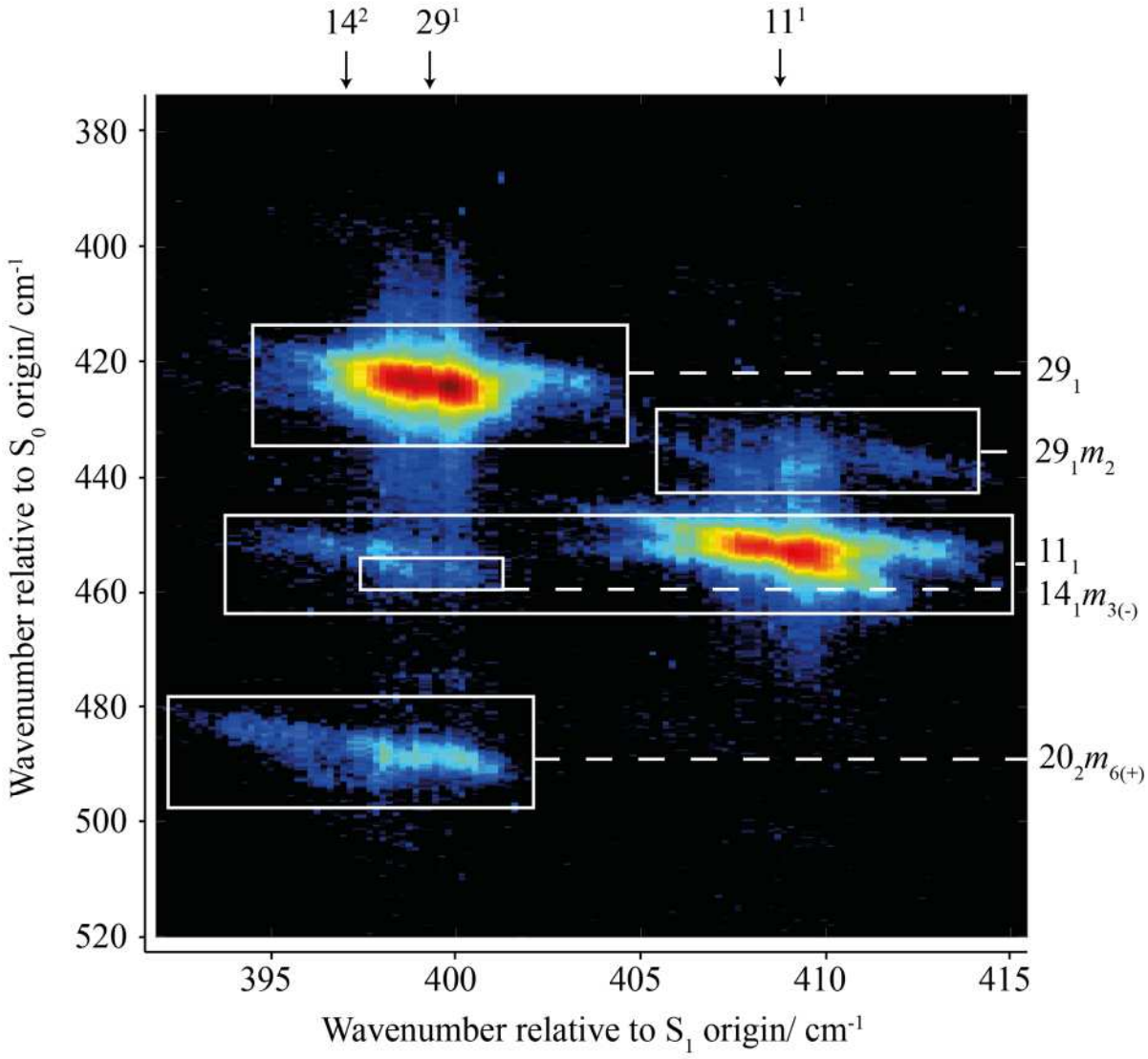
14²
29¹
11¹
380
400
420
440
460
480
500
520
395
400
405
410
415
Wavenumber relative to S0 origin/ cm-1
Wavenumber relative to S1 origin/ cm-1
29₁
29₁m₂
11₁
14₁m3(-)
20₂m6(+)

Figure 7

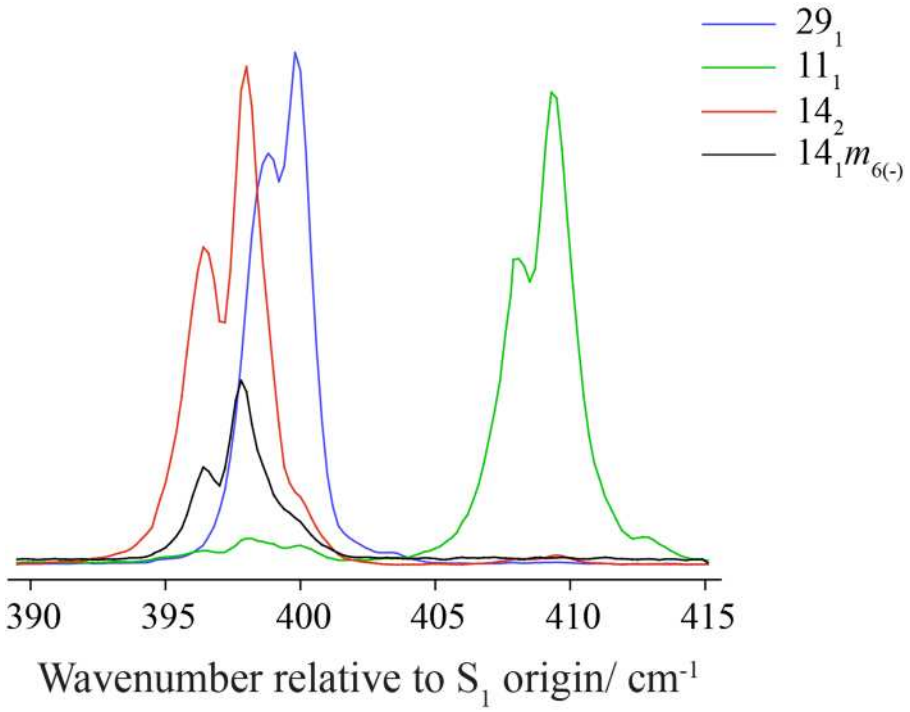
29_1
11_1
14_2
$14_1^2 m_{6(-)}$
390
395
400
405
410
415
Wavenumber relative to S_1 origin/ cm^{-1}

Figure 8

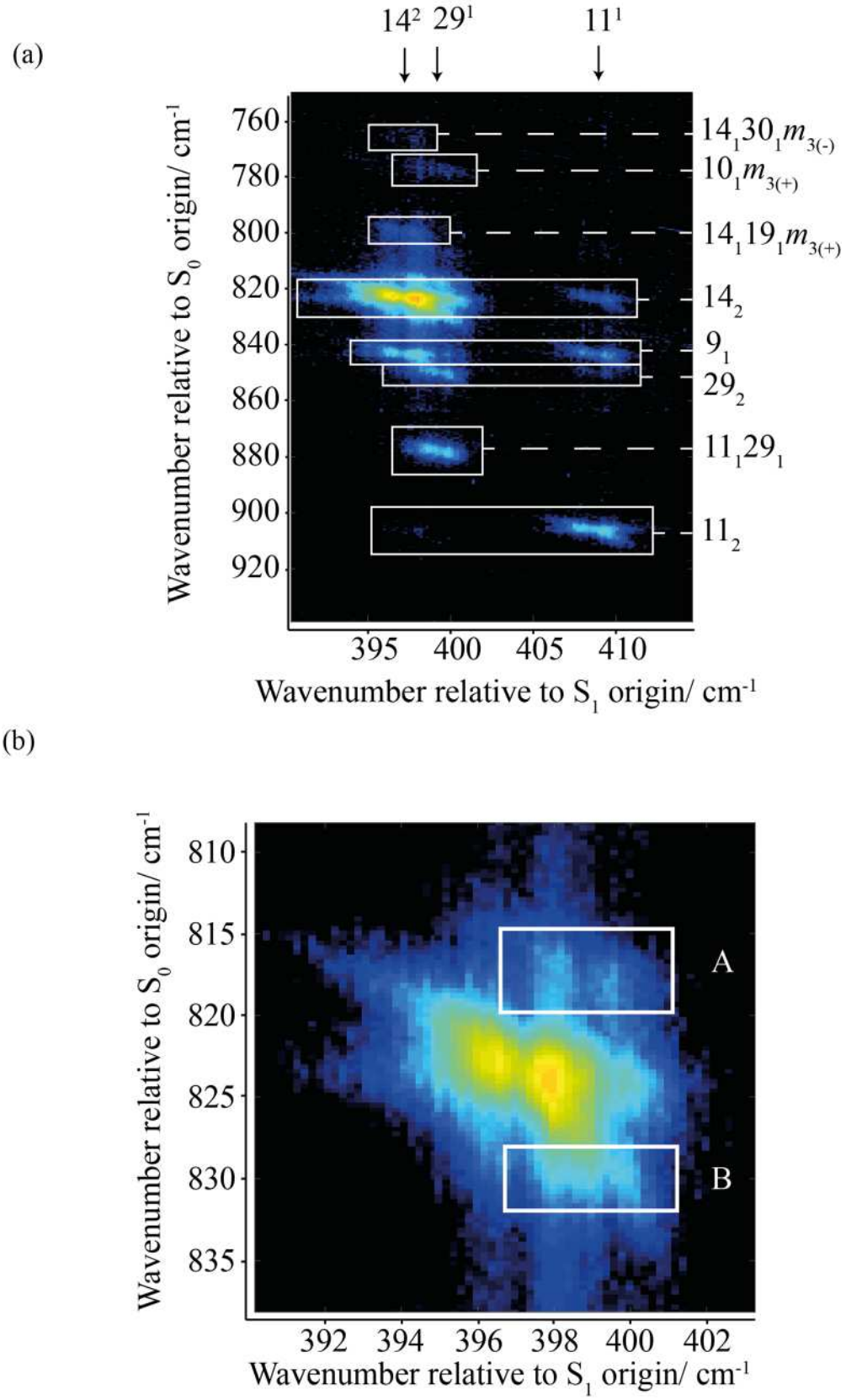
(a)
14² 29¹
11¹
760
780
800
820
840
860
880
900
920
Wavenumber relative to S0 origin/ cm-1
14130 1m3(-)
101m3(+)
14119 1m3(+)
142
91
292
11129 1
112
395
400
405
410
Wavenumber relative to S1 origin/ cm-1
(b)
810
815
820
825
830
835
Wavenumber relative to S0 origin/ cm-1
A
B
392
394
396
398
400
402
Wavenumber relative to S1 origin/ cm-1

Figure 9

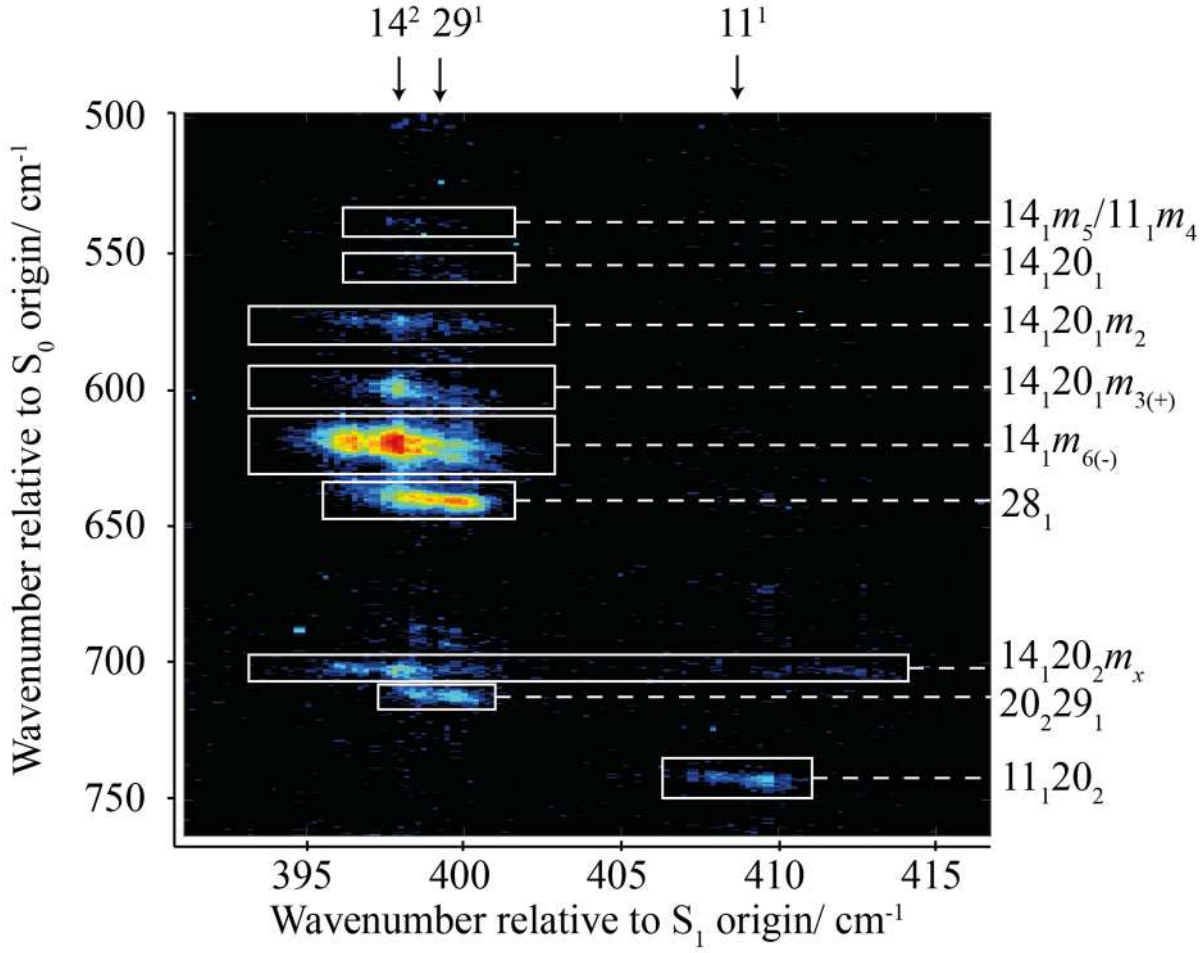
14² 29¹
11¹
500
550
600
650
700
750
Wavenumber relative to S0 origin/ cm-1
395
400
405
410
415
Wavenumber relative to S1 origin/ cm-1
14₁m₅/11₁m₄
14₁20₁
14₁20₁m₂
14₁20₁m₃(+)
14₁m₆(-)
28₁
14₁20₂mx
20₂29₁
11₁20₂

Figure 10

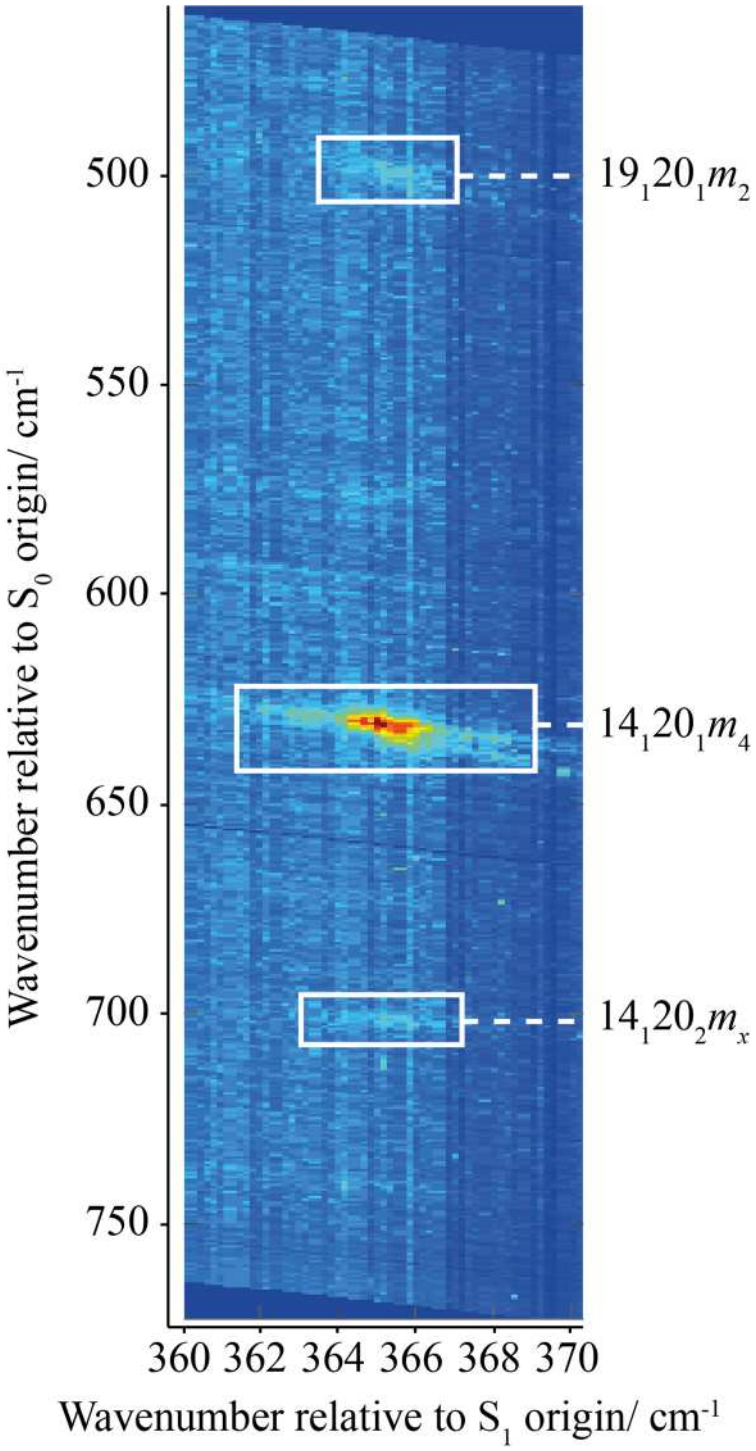
500
550
600
650
700
750
Wavenumber relative to S_0 origin/ cm^{-1}
$19_1 20_1 m_2$
$14_1 20_1 m_4$
$14_1 20_2 m_x$
360 362 364 366 368 370
Wavenumber relative to S_1 origin/ cm^{-1}

Figure 11

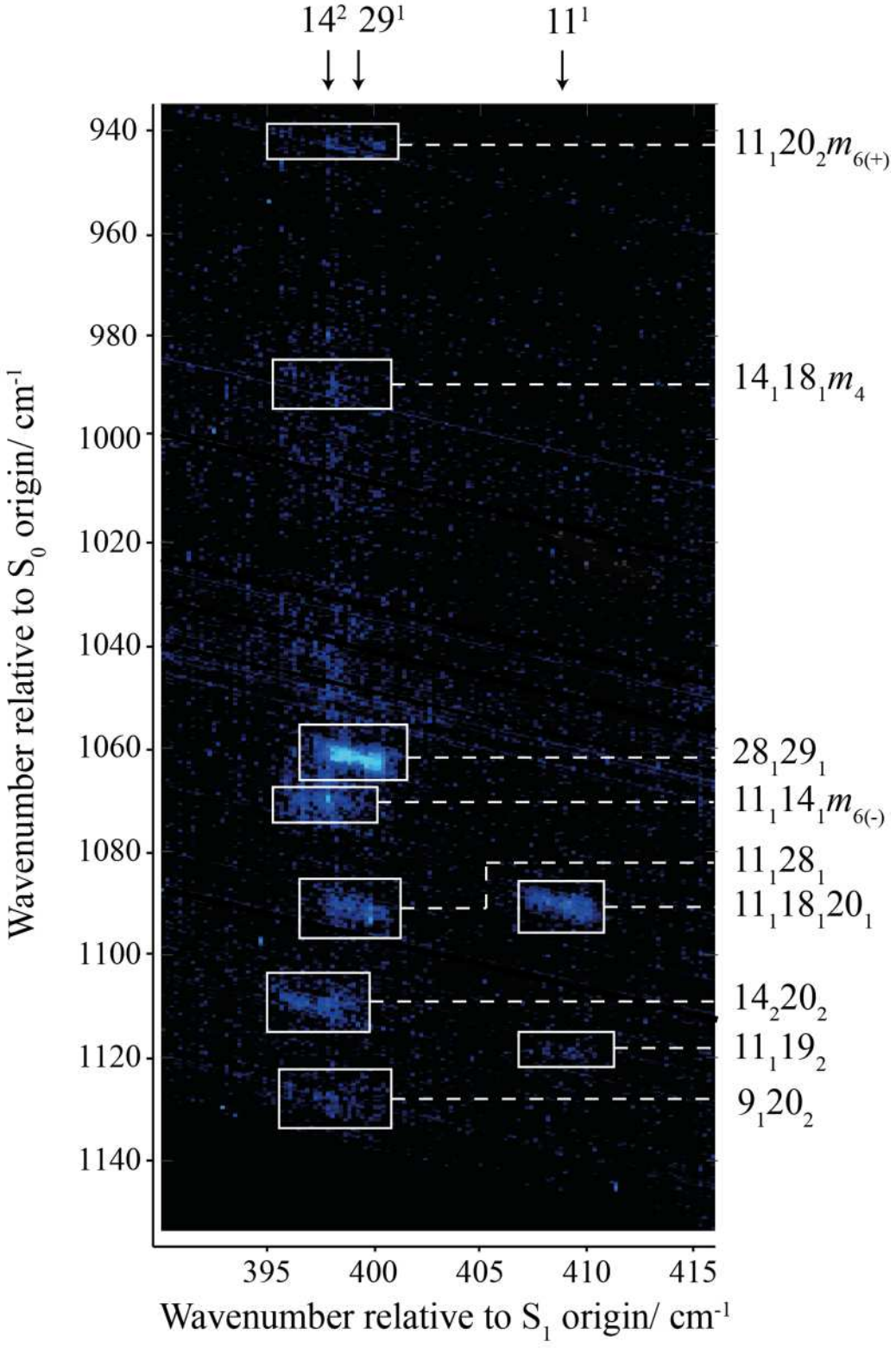
14² 29¹
11¹
940
960
980
1000
1020
1040
1060
1080
1100
1120
1140
Wavenumber relative to S0 origin/ cm-1
11120₂m6(+)
14118₁m4
28129₁
11114₁m6(-)
11128₁
11118₁20₁
14220₂
11119₂
9120₂
395
400
405
410
415
Wavenumber relative to S1 origin/ cm-1

Figure 12

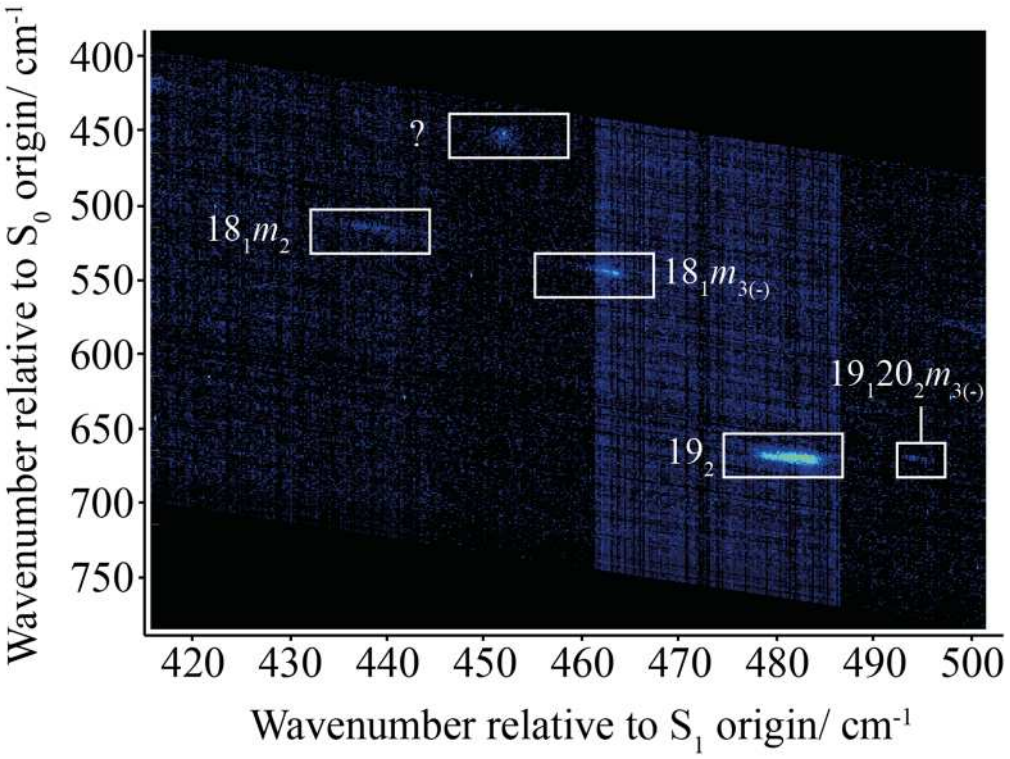
Wavenumber relative to S_0 origin/ cm^{-1}
400
450
500
550
600
650
700
750
?
18_1m_2
$18_1m_{3(-)}$
$19_120_2m_{3(-)}$
19_2
420
430
440
450
460
470
480
490
500
Wavenumber relative to S_1 origin/ cm^{-1}

Figure Captions

Figure 1: The 390–415 cm^{-1} region of the $S_1 \leftarrow S_0$ excitation spectrum of *p*FT recorded by (a) REMPI spectroscopy and (b) by vertical integration of the 2D-LIF spectrum across the emission range 350–890 cm^{-1}. The 14^2 and 29^1 bands overlap – see text.

Figure 2: Overview of the main region of the 2D-LIF spectra recorded in the present work. The spectral intensities are represented by colours, with red being the most intense through to blue being the least; black represents the zero background.

Figure 3: Expanded view of the DF spectrum of *p*FT in the 0–390 cm^{-1} region exciting via the origin, and the eigenstates dominated by 29^1, 14^2 and 11^1. This region covers the main torsion and vibtor levels associated with the D_{20}, D_{19} and D_{30} vibrations. The appearance of the spectrum via the origin is very similar to that recently published by Gascooke et al. in Ref. 16, where it is discussed in detail.

Figure 4: Expanded view of the DF spectrum of *p*FT in the 390–1090 cm^{-1} region exciting via the origin, and the eigenstates dominated by 29^1, 14^2 and 11^1. Selected assignments are shown and the spectrum is discussed further in the text together with the 2D-LIF spectra. Note that for the feature marked $14_1 20_2 m_x$, x may be 1 and/or 2 – see Section 3.4.3.3. Note that the 14^2 and 29^1 bands overlap and so the respective DF spectra contain small contributions from the overlapped feature.

Figure 5: Expanded view of the DF spectrum of *p*FT in the 1090–1390 cm^{-1} region exciting via the origin, and the eigenstates dominated by 29^1, 14^2 and 11^1. Selected assignments are shown and the spectrum is discussed further in the text together with the 2D-LIF spectra. Note that the 14^2 and 29^1 bands overlap and so the respective DF spectra contain small contributions from both levels.

Figure 6: Expanded view of the 2D-LIF spectrum covering the main $\Delta(v, m) = 0$ regions, (29^1, 29_1) and (11^1, 11_1). The approximate positions of the origins of the 14^2, 29^1 and 11^1 excitations are indicated at the top of the spectrum. The spectral intensities are represented by colours, with red being the most intense through to blue being the least; black represents the zero background.

Figure 7: Partial LIF spectra obtained by integrating across regions four $\Delta(v, m) = 0$ bands: 14^2, 29^1, $14^1 m^{6(-)}$ and 11^1 – see text. Note that the integrations were carried out over a vertical slice that included the main central activity of each band, and owing to different band shapes, and the need to avoid contributions from other features, these slices were not of the same height and so the results would not be accurately representative of relative intensities; thus, we have scaled three of these to the same maximum intensity, and one to half of their intensity for presentational reasons.

Figure 8: (a) Expanded view of the 2D-LIF spectrum covering the main (14^2, 14_2) $\Delta(v, m) = 0$ regions, and also (11^1, 11_2), (29^1, 29_2) and (29^1, $11_1 29_1$). The approximate positions of the origins of the 14^2, 29^1 and 11^1 excitations are indicated at the top of the spectrum. (b) Further expanded view showing the two extra features close to the (14^2, 14_2) band marked A and B – see text. The spectral intensities are represented by colours, with red being the most intense through to blue being the least; black represents the zero background.

Figure 9: Expanded view of the 2D-LIF spectrum covering the main ($14^1m^{6(-)}$, $14_1m_{6(-)}$) $\Delta(v, m) = 0$ regions, and also (29^1, 28_1). The approximate positions of the origins of the 14^2, 29^1 and 11^1 excitations are indicated at the top of the spectrum. Note that for the feature marked $14_120_2m_x$, x may be 1 and/or 2 – see text. The spectral intensities are represented by colours, with red being the most intense through to blue being the least; black represents the zero background.

Figure 10: Expanded view of the 2D-LIF spectrum covering excitation of the $S_10^0 + 364$ cm^{-1} band. Note that for the feature marked $14_120_2m_x$, x may be 1 and/or 2 – see text. The spectral intensities are represented by colours, with red being the most intense through to blue being the least; on this scale the zero background appears as a pale blue. Note that the triangular regions at the top right and bottom left of the image are unscanned regions.

Figure 11: Expanded view of the 2D-LIF spectrum covering the higher-wavenumber range 940–1140 cm^{-1}. The approximate positions of the origins of the 14^2, 29^1 and 11^1 excitations are indicated at the top of the spectrum. The spectral intensities are represented by colours, with red being the most intense through to blue being the least; black representing the zero background.

Figure 12: Expanded view of the 2D-LIF spectrum covering the excitation wavenumber range $S_10^0 +$ 420–500 cm^{-1}. The spectral intensities are represented by colours, with red being the most intense through to blue being the least; black represents the zero background in most areas, but between 460–485 cm^{-1} there is a region where the background is different, and appears as pale blue. Note that the triangular regions at the top right and bottom left of the image are unscanned regions. Tentative suggested assignments for the band marked '?' are given in the text.